JOURNAL
OF THE
WASHINGTON ACADEMY OF SCIENCES

VOL. 31 NOVEMBER 15, 1941 No. 11

MATHEMATICS.—*Intuitive and descriptive geometry of function space: Metric properties and transformation of coordinates.*[1] BRUCE LONGTIN, Department of Chemistry, Illinois Institute of Technology, and MERLE RANDALL, Department of Chemistry, University of California. (Communicated by FREDERICK D. ROSSINI.)

In a previous paper[2] a graphical method of representing spaces of an indefinitely large number of dimensions was developed. The method consists essentially in dividing an interval Δ into n equal subintervals and erecting an ordinate equal to one of the vector components (i.e., Cartesian coordinate numbers) at the center of each subinterval. A number of geometrical figures were studied descriptively by the use of this representation.

In everyday 3-space, geometric intuitions are developed through the ability to survey an object from many viewpoints; to pick it up, turn it around, and move it back and forth. These operations of rotation and translation enable one who can see only two dimensions at a time to appreciate the geometry of a third dimension. The significant result of such geometrical observations is the conclusion that certain geometric features of an object, such as lengths and angles, remain unaltered by rotation and translation. It is this property that gives meaning to the operation of geometrical measurement.

The analytic aspects of the metric properties of function space form one of the most thoroughly investigated fields of functional theory. For this reason the analytical results will be presented as briefly as possible except where clarification is necessary.

SCALAR PRODUCT OF TWO VECTORS

The scalar product $\mathbf{u}\cdot\mathbf{v}$ of the vectors $\mathbf{u}$ and $\mathbf{v}$ is defined geometrically as the product of their lengths $|u|$ and $|v|$ times the cosine of the angle θ between the two vectors;

$$\mathbf{u}\cdot\mathbf{v} = |u||v| \cos\theta. \tag{1}$$

[1] Clerical assistance of the Work Projects Administration is gratefully acknowledged. O.P. 165-1-08-73. (Unit C-2.) Received July 22, 1941.

[2] RANDALL and LONGTIN. *Intuitive and descriptive geometry of function space: The graphical representation of geometrical figures.* Journ. Washington Acad. Sci. 31(10): 421–431. 1941.

If the two vectors **u** and **v** are identical, the angle between them is zero and cos θ is unity. In this case, the scalar product $\mathbf{u}\cdot\mathbf{u}$ is the square of the length of the single vector;

$$\mathbf{u}\cdot\mathbf{u} = |u|^2. \tag{2}$$

Since the scalar product may be evaluated by methods that are independent of any previous knowledge of the length of the vectors, equation 2 permits an analytic evaluation of the length of any vector. Equation 1 may then be solved for the angle θ between two vectors, in the form

$$\cos\theta = \mathbf{u}\cdot\mathbf{v}/|u||v|, \tag{3}$$

or

$$\theta = \cos^{-1}[\mathbf{u}\cdot\mathbf{v}/|u||v|]. \tag{4}$$

Thus the metric properties of any Euclidean space may be expressed in terms of the scalar products of vectors. Such an expression is much simplified by introducing the general vector notations.

Base vector systems.—An orthogonal set of vectors consists of vectors mutually perpendicular. The scalar product of any two vectors of such a set is zero ($\cos 90° = 0$), as indicated by equation 1, unless the two are identical. A normalized set of vectors consists of vectors each of which is of unit length. An *orthonormal* set is both orthogonal and normalized. If the vectors $\mathbf{e}_i^0, \mathbf{e}_j^0, \cdots$, form an orthonormal set, they satisfy the equation

$$\mathbf{e}_i^0\cdot\mathbf{e}_j^0 = \delta_{ij}, \tag{5}$$

where δ_{ij} (Kronecker's delta symbol) is zero except in the case that i and j are identical; then it takes the value unity.

In Euclidean spaces of a finite number of dimensions, any vector **v** is readily expressed in terms of an orthonormal set $\mathbf{e}_i^0, \mathbf{e}_j^0, \cdots$, in the form

$$\mathbf{v} = v_1\mathbf{e}_1^0 + v_2\mathbf{e}_2^0 + \cdots + v_n\mathbf{e}_n^0 = \sum_1^n v_i\mathbf{e}_i^0, \tag{6}$$

the coefficients $v_i, v_j, \cdots$ being scalar quantities. The set of vectors $\mathbf{e}_i^0, \mathbf{e}_j^0, \cdots$ is then called a *base vector system.* Any system of vectors may be used as a base vector system provided the number of base vectors is the same as the number of dimensions of the space under consideration, while no one of the base vectors may be expressed in terms of the others by any equation such as equation 6.

If the vectors **u** and **v** have been represented in terms of the same

orthonormal base vector system, $\mathbf{e}_i^0$, $\mathbf{e}_j^0$, $\cdots$, their scalar product takes the form

$$\mathbf{u}\cdot\mathbf{v} = \left(\sum_1^n u_i\cdot\mathbf{e}_i^0\right)\cdot\left(\sum_1^n v_j\mathbf{e}_j^0\right) = \sum_{i=1}^n\sum_{j=1}^n u_iv_j\mathbf{e}_i^0\cdot\mathbf{e}_j^0. \tag{7}$$

Recalling equation 5, we see that this result may be reduced to the simple form

$$\mathbf{u}\cdot\mathbf{v} = u_1v_1 + u_2v_2 + \cdots + u_nv_n = \sum_{i=1}^n u_iv_i. \tag{8}$$

Two special cases are of interest. If the vector $\mathbf{u}$ is one of the base vectors, $\mathbf{e}_i^0$, then the coefficients $u_1, u_2, \cdots, u_n$ are all zero except u_i, which is unity. In this case, the scalar product

$$\mathbf{e}_i^0\cdot\mathbf{v} = v_i \tag{9}$$

is the length of the vector $\mathbf{v}$ times unity times the cosine of the angle between $\mathbf{v}$ and the base vector $\mathbf{e}_i^0$. Thus the coefficient v_i is the length of the projection of the vector $\mathbf{v}$ on the axis of the vector $\mathbf{e}_i$; it is the vector component in this direction. If the vectors $\mathbf{u}$ and $\mathbf{v}$ are identical, one obtains the formula

$$\mathbf{u}\cdot\mathbf{u} = u_1^2 + u_2^2 + \cdots + u_n^2, \tag{10}$$

which is the ordinary Euclidean expression for the square of the length of the vector $\mathbf{v}$.

From equation 10 it is evident that the length of the vector $\mathbf{u}$ will approach an infinite value as the number of dimensions is increased indefinitely, if each component has a finite value. If all components of the vector have the same order of magnitude, the length of the vector will approach a finite limit only if the individual components are of infinitesimal length.

Such vectors, whose components are of infinitesimal length, are of great importance in the geometry of function space. They are best represented in terms of a *reduced base vector system* defined by the equation

$$\mathbf{e}_i' = (\Delta/n)^{1/2}\mathbf{e}_i^0. \tag{11}$$

The vectors of the reduced system are orthogonal but are not normalized. They have the same directions as vectors of the orthonormal set, but each has a length $(\Delta/n)^{1/2}$ rather than unity. This length approaches an infinitesimal value as the number, n, of dimensions increases.

The quantity (Δ/n) is the width of each of the n subintervals into which the interval Δ is subdivided in order to construct the block

diagram representation of an n-space vector. When the number of subdivisions becomes infinite, (Δ/n) may be replaced by its equivalent, dx. Here x denotes the distance[3] $(a+(i/n)\Delta)$, whose increment is (Δ/n) when the index i increases by unity. In this case equation 11 takes the form

$$\mathbf{e}_i' = (dx)^{1/2}\mathbf{e}_i^0. \tag{12}$$

In order to represent the vector $\mathbf{v}$ in terms of the reduced base vector system, new components, v_i', must be defined which are $(1/dx)^{1/2}$ times as big as the original components:

$$v_i' = v_i/(dx)^{1/2} \tag{13}$$

and hence may be finite rather than infinitesimal.[4] Equation 6 then takes the form

$$\mathbf{v} = v_1'\mathbf{e}_1' + v_2'\mathbf{e}_2' + \cdots + v_n'\mathbf{e}_n' = \sum_1^n v_i'\mathbf{e}_i'. \tag{14}$$

Scalar product in Hilbert space.—A Euclidean space of an infinite number of dimensions is known as a Hilbert space.[5] By using the reduced base vector system for such a space, equation 8 becomes the sum of an infinite number of terms $u_i'v_i'(\Delta/n)$, whose limit is the integral

$$\mathbf{u}\cdot\mathbf{v} = \int_a^{a+\Delta} u'(x)v'(x)dx. \tag{15}$$

In this equation, the subscript i has been replaced by the variable x, which is $[a+(i/n)\Delta]$. The square of the length of any vector in Hilbert space is thus given as

$$|u|^2 = \mathbf{u}\cdot\mathbf{v} = \int_a^{a+\Delta} [u'(x)]^2dx. \tag{16}$$

Angle between two vectors.—The scalar product $\mathbf{u}\cdot\mathbf{v}$ and the two lengths $|u|$ and $|v|$ appearing in equation 4 may be evaluated with the help of equations 15 and 16. Proceeding in this way, Frank and Pick[6] have made a rather detailed study of the spherical geometry of function space. Their valuable work on the angles which

[3] RANDALL and LONGTIN. *Op. cit.*

[4] Cf. KOWALEWSKI, G. *Ueber Funktionenräume*, Sitz. Akad. Wien **120**(2a: 1): 77. 1911. Kowalewski obtains this result without mentioning the role of the base vector system.

[5] HILBERT, DAVID. *Grundzüge einer allgemeinen Theorie der linearen Integralgleichungen*, Leipzig and Berlin, 1912, a collection from Gött. Nachr. **1904**: 49, 213; **1905**: 307; **1906**: 157, 439; **1910**: 355.

[6] FRANK and PICK. Math. Ann. **76**: 354. 1915. PICK. Compt. Rend. **158**: 549. 1914. These two papers contain the only cases found in which the geometrical representation of vectors in function space has actually been used.

may exist between "convex" functions need not be repeated here.

As one interesting application, consider the angle between a vector $\mathbf{v}$ whose length $|v|$ is unity, and one of the orthonormal base vectors, $\mathbf{e}_i^0$. In the formulas, the vector $\mathbf{u}$ may be replaced by $\mathbf{e}_i^0$. Both of the lengths $|u|$ and $|v|$ of equation 9 are unity. In accordance with equation 9, the scalar product $\mathbf{e}_i^0 \cdot \mathbf{v}$ must have the value v_i, equal to $v_i'(dx)^{1/2}$, and this result is obtained from equation 16 when the integration is carried out properly. Consequently,

$$\theta = \cos^{-1} [v_i'(dx)^{1/2}] \sim [\pi/2 - v_i'(dx)^{1/2}]; \qquad (17)$$

the angle θ deviates only slightly from 90°, or $\pi/2$ radians, provided the component v_i' is finite.

In the previous paper,[7] we chose to represent a vector in function space by means of a continuous (or piecewise continuous) curve with no infinite ordinates. The function $v'(x)$ representing the vector $\mathbf{v}$ is in this case continuous and finite. Consequently every reduced component v_i' of the vector $\mathbf{v}$ is finite, and the angle θ that it makes with every vector of the base vector system is nearly 90°.

In 2-dimensional space there is no region that is nearly 90° away from both axes. The closest approach to such a region is one lying at about 45° away from both axes. In 3-space a region may be found that lies about 55° away from all three axes. As the number of dimensions increases, the angle between a base vector and the vector that makes equal angles with all base vectors increases toward 90°. With an infinite number of dimensions there is a great abundance of space in the region *nearly* 90° away from all the coordinate axes (base vectors). Such an abundance of space will be noticed repeatedly in regions of function space which in analogy to common 3-dimensional experience would at first seem insignificant.

The integrating vector.—A vector all of whose components are zero or unity in terms of the reduced base vector system has peculiarly important properties. Let the subscript E denote the ensemble (or collection) of indices for which the components of such a vector have the values unity rather than zero. The vector having these components is designated as $\mathbf{e}_E$. In particular, when the components are zero for all indices except those between b and c and unity for all indices in this interval (inclusive of b and c), the vector will be designated as $\mathbf{e}_b^c$. Such a vector is represented in Fig. 1 by the method previously developed, in which the vector components are plotted as ordinate against the indices (scale $1/n$ = unity) as abscissa.

[7] RANDALL and LONGTIN. *Op. cit.*

The scalar product $\mathbf{e}_b{}^c \cdot \mathbf{v}$ proves to be simply the integral

$$\mathbf{e}_b{}^c \cdot \mathbf{v} = \int_b^c v'(x)dx, \tag{18}$$

extended over the interval from b to c. This is evident when one substitutes for $u'(x)$ in equation 15 the components of $\mathbf{e}_b{}^c$, which are zero except in the interval (bc) and unity within this interval. In a more general sense,[8] the scalar product $\mathbf{e}_E \cdot \mathbf{v}$ is the integral of $v(x)$ over the ensemble of values of x included in E. Because of the role which the vector $\mathbf{e}_E$ may be considered to play in the theories of integration, we may designate it as the *integrating vector*.

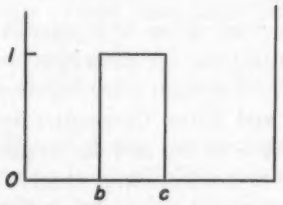

Fig. 1.—A vector all of whose components between indices b and c are unity. (Scale, $1/n$ = unity.)

In the previous paper[9] the phase diagrams of complex chemical mixtures were given as an example of the application of the methods therein developed. When the mixture is that of a series of hydrocarbons and other volatile substances, the index i is taken as the "true boiling point," Θ, of the component substance. The original data from which the analysis of the mixture is obtained give the total weight of material whose true boiling point is less than Θ. The desired analysis gives the weight of substance boiling between Θ and $\Theta + d\Theta$. If $W(\Theta)$ represents the total weight boiling below Θ, and $w(\Theta)d\Theta$ the desired value[10]

$$W(\Theta) = \mathbf{e'}_0{}^{\Theta} \cdot \mathbf{w} = \int_0^{\Theta} w(\Theta)d\Theta. \tag{19}$$

The weights of the individual components, which are used as the vector components in the phase diagram, are therefore obtained as

$$w(\Theta) = dW/d\Theta. \tag{20}$$

This serves to indicate another manner in which the representation

[8] Compare Lebesgue integration; LEBESGUE, *Leçons sur l'intégration*, Paris, Gauthier-Villars, 1928.

[9] RANDALL and LONGTIN. *Op. cit.*

[10] Here and subsequently it will be assumed that the reduced base vector system is to be used, and the designation by accents omitted except where confusion may arise.

in function space may arise. Usually in this case the condition $\mathbf{e}'_0{}^{\infty} \cdot \mathbf{w} = 1$ is also imposed so that $w(\Theta)$ represents the weight fraction rather than total weight of the component.

Orthonormal vector sets.—Consider an orthonormal set of vectors $\mathbf{e}_\alpha{}^0, \mathbf{e}_\beta{}^0, \cdots, \mathbf{e}_\nu{}^0$, different from the base vector system $\mathbf{e}_1{}^0, \mathbf{e}_2{}^0, \cdots, \mathbf{e}_n{}^0$. Each vector $\mathbf{e}_\lambda{}^0$ of this set can be represented in terms of the reduced base vector system as the sum of its components $e_{\lambda i}'\mathbf{e}_i'$. The coefficient $e_{\lambda i}'$ is the magnitude of the reduced component of $\mathbf{e}_\lambda{}^0$ in the direction of the base vector $\mathbf{e}_i{}^0$. In the limit of an infinite number of dimensions, this coefficient becomes a function $e_\lambda'(x)$, which may be used to represent the vector graphically by the method previously discussed.

If the vectors $\mathbf{e}_\alpha{}^0, \mathbf{e}_\beta{}^0, \cdots, \mathbf{e}_\nu{}^0$ form an orthonormal set, they must satisfy a relationship like equation 5. Expressed in the form appropriate to function space, this requires that

$$\mathbf{e}_\kappa{}^0 \cdot \mathbf{e}_\lambda{}^0 = \int_a^{a+\Delta} e_\kappa'(x) e_\lambda'(x) dx = \delta_{\kappa\lambda} \tag{21}$$

for all pairs of subscripts κ, λ. A set of functions $e_\alpha'(x), e_\beta'(x), \cdots, e_\nu'(x)$ that satisfy equation 21 are said to be orthogonal and normalized with respect to the interval Δ; this is not necessarily true with respect to any other interval of the variable x. An example is the set of functions $(1/\Delta)^{1/2}$, $(2/\Delta)^{1/2} \sin(\theta)$, $(2/\Delta)^{1/2} \cos(\theta)$, $(2/\Delta)^{1/2} \sin(2\theta)$, $(2/\Delta)^{1/2} \cos 2\theta$, $(2/\Delta)^{1/2} \sin 3\theta, \cdots$, where θ has the value $2\pi x/\Delta$. The functions of this set are all orthogonal[11] and normalized with respect to any interval of width Δ but of no other width.

Transformation of axes.—Since the set of vectors $\mathbf{e}_\alpha{}^0, \mathbf{e}_\beta{}^0, \cdots, \mathbf{e}_\nu{}^0$ are orthonormal, they may serve equally as well for a base vector system as the original set $\mathbf{e}_1{}^0, \mathbf{e}_2{}^0, \cdots, \mathbf{e}_n{}^0$. The components of a vector $\mathbf{v}$ were represented in the original system by the function $v'(x)$. In the new system the values of the components are found with the help of equations 9, 12, and 13 as

$$v_\lambda' = \mathbf{v} \cdot \mathbf{e}_\lambda' = \int_a^{a+\Delta} v'(x) e_\lambda'(x) dx. \tag{22}$$

As an example, the vectors $\mathbf{e}_\lambda{}^0$ may be those whose representative functions, $e_\lambda'(x)$, are terms of the sine and cosine series discussed above. In this case the component v_λ' will be recognized as the coefficient of $e_\lambda'(x)$ in the Fourier series expansion for $v'(x)$.

If the system $\mathbf{e}_\alpha{}^0, \mathbf{e}_\beta{}^0, \cdots, \mathbf{e}_\nu{}^0$ is to serve as a complete base vector

[11] See COURANT. *Differential and integral calculus* 1: chapter 9. 1939.

system in function space the number, n, of vectors in the set must be infinite. To represent a vector $\mathbf{v}$ graphically in terms of the new system, an interval Δ' (not necessarily the same as Δ) is divided into n subintervals. At the center of the λth interval an ordinate of height v_λ' is erected (for all values of λ). In the limit, the subscript λ may be replaced by a continuous variable ξ, whose value is $[a'+(\lambda/n)\Delta']$. The vector $\mathbf{v}$ is then represented in the new system by a function $v'(\xi)$, not the same as the function $v'(x)$.

For example, consider the vector $\mathbf{v}$ which is represented in terms of the system $\mathbf{e}_1^0, \mathbf{e}_2^0, \cdots, \mathbf{e}_n^0$ by the curve and three isolated points of Fig. 2.

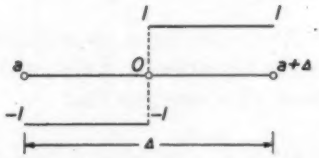

Fig. 2.—The vector $\mathbf{v}$ represented in the system $\mathbf{e}_1^0, \mathbf{e}_2^0, \cdots, \mathbf{e}_n^0$.

A new base vector system $\mathbf{e}_\alpha^0, \mathbf{e}_\beta^0, \cdots, \mathbf{e}_\nu^0$ is represented in terms of the old by means of the Fourier series terms listed above. The

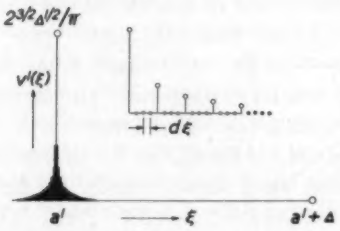

Fig. 3.—The same vector $\mathbf{v}$ (Fig. 2) represented in terms of a new coordinate system $\mathbf{e}_\alpha^0, \mathbf{e}_\beta^0, \cdots, \mathbf{e}_\nu$. In the inset the ξ-axis has been infinitely magnified to show the details close to the point $\xi = a'$. The actual width of the shaded block at a' is infinitesimal.

Fourier coefficients of the function $v'(x)$ of Fig. 2 are all zero except those of the odd-numbered sine terms. If the normalized functions are used, the coefficients of these sine terms are $(2^{3/2}\Delta^{1/2}/\pi\kappa)$ where κ is the (odd) number of the sine term, counting sine terms only. These are the vector components, $\mathbf{v}_\lambda$. Let j denote the number of the term in the order listed previously, and define the variable ξ as $[a'+(j/n)\Delta']$ where n is the total number of all terms. Then the vector components v_λ are represented by a function $v(\xi)$, which has alternately the values

zero and $(2^{5/2}\Delta^{1/2}/\pi)[d\xi/(\xi-a')]$. Between each pair of points for which its value is definite are three points for which the value is zero.

The function $v(\xi)$ obtained in this manner is shown in Fig. 3. It has finite values only as long as $(\xi-a')/d\xi$ remains a denumerable quantity. After $(\xi-a')d\xi$ reaches an infinite value (not denumerable) the remaining values of $v(\xi)$ differ only infinitesimally from zero. With an infinite (not denumerable) number of dimensions, this point is reached before ξ differs from a' by more than an infinitesimal amount, as indicated in the figure.

In this example, the new coordinate system contains several axes [those represented by $(2/\Delta)^{1/2}\sin\theta$, $(2/\Delta)^{1/2}\sin 3\theta$, and $(2/\Delta)^{1/2}\sin 5\theta$ in particular] that lie in nearly the same region of function space as does the vector **v**. This is evidenced in par' by the similarity in form between the function representing any one of these base vectors and that representing **v** [which is *crudely* sinusoidal]. Consequently the vector **v**, as represented in the new coordinate system, has important components only in these few directions; the function $v'(\xi)$ has non-zero values for a few values of ξ.

The transformation from one orthonormal base vector set to a second in Hilbert space leaves the scalar product of any two vectors unaltered. Consequently, the length of a vector and the angle between two vectors are quantities that may be calculated in the same way and with the same answer, regardless of the base vector system used in describing the vectors. Thus, for example, the length of the vector **v** obtained by applying equation 16 will be the same whether the function $v'(x)$ and variable x or the function $v'(\xi)$ and variable ξ are used. The area under the curve obtained by squaring the ordinate of Fig. 2 is the same as that under the block diagram obtained by squaring the ordinates of Fig. 3.

AUXILIARY PROJECTIONS

In the previous paper[12] it was shown that a desired principle projection of function space into two or three dimensions is obtained by constructing a 2- or 3-dimensional figure with Cartesian coordinates equal to values from the complete vector diagram corresponding to the desired two or three particular indices of the set x.

In the practice of descriptive geometry the use of auxiliary projections is quite helpful. The auxiliary projection may be considered as a principle projection relative to a coordinate system whose orientation is different from the original coordinate system. In function

[12] RANDALL and LONGTIN. *Op. cit.*

space, the auxiliary projection may be obtained by representing the geometrical figure in terms of a new coordinate system $\mathbf{e}_\alpha{}^0$, $\mathbf{e}_\beta{}^0$, $\cdots$, $\mathbf{e}_\nu{}^0$, taking it as a principal projection relative to the new representation. Thus the transformation of axes by the methods discussed above affords a new point of view from which to survey the function space figure by means of projections.

For example, one may study the configuration of two intersecting straight lines $(\mathbf{r}+s\mathbf{u})$ and $(\mathbf{r}+t\mathbf{v})$ by looking at it from all possible angles. In other words, its principal 2-dimensional projection will be taken with respect to every different possible base vector system. These projections will all show two intersecting straight lines, with varying degrees of foreshortening of lengths and angles. They are like the various aspects obtained by looking at a pair of intersecting lines from different directions in ordinary 3-space.

Of all the different aspects of a plane figure, the most important is that which looks directly at the plane, so that the figure shows no foreshortening. To obtain this projection one makes use of axes consisting of two mutually perpendicular lines lying in the plane and other axes perpendicular to the plane and each other. These other axes are unimportant, since they are to be suppressed in taking the projection.

In applying the method to the two intersecting lines, it is convenient to choose as the axes lying in the plane one of the two lines, and a second perpendicular to it. It may be shown that the component of a vector $\mathbf{v}$ parallel to the vector $\mathbf{u}$ is given by the expression $[\mathbf{u}(\mathbf{v}\cdot\mathbf{u})/(\mathbf{u}\cdot\mathbf{u})]$. Consequently the expression $[\mathbf{v}-\mathbf{u}(\mathbf{v}\cdot\mathbf{u})/(\mathbf{u}\cdot\mathbf{u})]$ gives the component of $\mathbf{v}$ perpendicular to $\mathbf{u}$. It must necessarily lie in the plane of $\mathbf{u}$ and $\mathbf{v}$, and is suitable for use as the second of the two axes. The ratio $(\mathbf{v}\cdot\mathbf{u})/(\mathbf{u}\cdot\mathbf{u})$ may be determined from equations 16 and 17 with the help of graphical integration, if the representative functions $u(x)$ and $v(x)$ are known. The function $u(x)$ is multiplied by this ratio and subtracted from $v(x)$ to construct a function representative of this second coordinate axis.

Fig. 4 (left) represents a radius vector $\mathbf{r}$ that extends to the intersection of vectors $\mathbf{u}$ and $\mathbf{v}$. In Fig. 4 (right vector $\mathbf{u}$ has been taken to give the direction of one coordinate axis while a second is taken along the component of $\mathbf{v}$ that is perpendicular to $\mathbf{u}$. The components of $\mathbf{v}$ and $\mathbf{r}$ along the directions of these two axes were obtained by the method that gives $[\mathbf{u}(\mathbf{v}\cdot\mathbf{u})/(\mathbf{u}\cdot\mathbf{u})]$ as the component of $\mathbf{v}$ parallel to $\mathbf{u}$. The projection of this figure taken normal to the plane of $\mathbf{u}$ and $\mathbf{v}$ was constructed from these vector components. In this figure, the lines $[\mathbf{r}+s\mathbf{u}]$ and $[\mathbf{r}+t\mathbf{v}]$ actually appear as intersecting lines. Furthermore

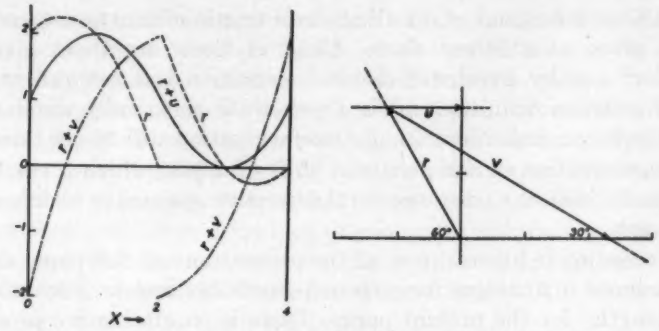

Fig. 4.—Normal projection of the intersection of two straight lines.

the angle of 30° between them is that calculated from the function $u(x)$ and $v(x)$ by equations 4, 15, and 16

Frank and Pick[13] have by similar means obtained a projection of the intersection of a plane and hypersphere, using the given plane as the plane of projection. The projection of course appears as a circle. Many similar exercises in projective geometry may be carried out by the same means.

NONORTHOGONAL AND NONEUCLIDEAN SYSTEMS

In ordinary descriptive geometry occasional use is made of oblique projections; in these the projection rays are not normal to the projection plane. Such projections are to be obtained by representing the figure in terms of a nonorthogonal base vector system of which one group defines the projection space, and the remaining group defines a space parallel to the projection elements. The desired projection is then obtained by suppressing the coordinates parallel to the projection elements, just as a principal orthogonal projection is obtained.

The transformation is most readily accomplished with the aid of the set of vectors reciprocal to the base vector set (i.e., if the base vector system is covariant, the other system is the corresponding contravariant system of vectors). The representative functions of these two base vector systems form what is known as a biorthogonal system. This transformation is not of sufficient importance to be described in detail.[14]

[13] FRANK and PICK. *Op. cit.*

[14] The equations of the transformation may be obtained as a generalization of the equations given in WILLS, *Vector tensor analysis*, §20, 1931, or any other text on the subject. The analytic generalization to function space is the subject of the following works: SCHMIDT, ERHARD, *Dissertation*, Gottingen, 1905; LEVY, P., *Leçons d'analyse fonctionnelle*, Gauthier-Villars, Paris, 1922; COURANT and HILBERT, *Methoden math. Physik. I.*, pp. 19, 34. Berlin, J. Springer, 1924.

Various definitions of non-Euclidean metric of function space have been given at different times. Chief of these are those given by Hölder[15] and by Fréchet.[16] Hölder's definition is a generalization of the Euclidean definition, while Fréchet's is generically unrelated to the Euclidean definition. In any case a rotation will be considered as a transformation of axes, without shift of origin, which preserves all the (non-Euclidean) distances in the function space save certain singular ones.

Proceeding in like manner, all the propositions of this paper may be reproduced in analogue for each non-Euclidean metric. Such a task is too lengthy for the present paper. There is an alternative procedure of studying non-Euclidean geometry that will be discussed further in a subsequent paper. It arises as a generalization of the transformation theory in tensor analysis. It has already been briefly discussed by Delsarte[17] in a series of papers on subgroups of the Fredholm transformation.

CONCLUSIONS

In function space purely mechanical methods of measurement and of shifting the orientation of figures are not possible. Analytical methods must be substituted. These methods have been collected. and some attempt has been made to give them physical significance. Equation 16 serves as the basis for measuring distances in function space, while equations 4, 15, and 16 serve to measure angles when the geometrical figures have been represented by the proposed method.

By representing the geometrical figure in terms of new coordinate systems, different oblique views are made available. The same transformation may serve a different purpose. The observer may imagine that he has changed his viewpoint to coincide with one axis (or more) of the new system. He might then grasp the coordinate axes, rotating them into coincidence with the old axes. If the geometrical figure moves with the axes, it will continue to be represented in terms of these moving axes by the same diagrams, although its representation in terms of the fixed axis system is changing. Hence the use of different axis systems allows one the freedom of either a movable observer or a movable object.

The chief methods of descriptive geometry are the construction of principal and auxiliary projections (including the normal projection), the construction of straight lines, and the location of intersections.

[15] HÖLDER. *Die mathematische methode*, Springer, Berlin, 1928.
[16] FRÉCHET. *Les espaces abstraits*, Gauthier-Villars, Paris, 1924.
[17] DELSARTE. Compt. Rend. 186: 415, 1095, 1412, 1513. 1928.

These methods have all been developed for function space in this and the preceding paper. Applications to special problems may be made in general by analogy to the ordinary 3-dimensional case.

Practical geometrical intuitions are developed by selecting from among all aspects of each geometrical figure those which are invariant. In Hilbert space, we have found that the angle between two lines and the length of a line are independent of the point of view. These invariant properties form a backlog of geometric intuition for function space, to which other more specialized intuitions may be added by studying many aspects of many geometrical figures. A few examples will be included in the following paper.

MATHEMATICS.—*Intuitive and descriptive geometry of function space: Geometric configurations.*[1] MERLE RANDALL, Department of Chemistry, University of California, and BRUCE LONGTIN, Department of Chemistry, Illinois Institute of Technology. (Communicated by FREDERICK D. ROSSINI.)

In two preceding papers[2,3] a graphical representation of spaces of an indefinite number of dimensions was developed, together with the concepts of Euclidean projection and rotation, which are fundamental to the descriptive geometry of such a space. In this paper the application of these methods to actual problems of descriptive geometry is indicated.

The analytic geometry of a number of relatively simple n-space figures has been well studied.[4] A number of these results will be needed in order to obtain a graphical representation of these figures.

CURVED LINES AND SURFACES

A space curve may be represented analytically either as the intersection of two surfaces, or by means of parametric equations that express the various coordinates as functions of a single parameter, s (e.g., the curvilinear distance from a fixed point on the curve). The analytic representation of an m-dimensional hypersurface is most readily obtained by expressing the n coordinates in terms of m independent parameters (i.e., the m parameters of the surface). These parametric equations are of the form

[1] Clerical assistance of the Works Project Administration is gratefully acknowledged. O. P. 165-1-08-73. (Unit C-2.) Received July 22, 1941.

[2] RANDALL and LONGTIN. Journ. Washington Acad. Sci. 31(10): 421–431. 1941.

[3] LONGTIN and RANDALL. Journ. Washington Acad. Sci. 31(11): 441–453. 1941.

[4] Cf. LEVY, P. *Leçons d'analyse fonctionnelle*, Paris, Gauthier-Villars, 1922.

$$v_i = f_i(t_1, t_2, \cdots, t_m); \quad i = 1, 2, \cdots, n \tag{1}$$

in which $t_1, t_2, \cdots, t_m$ are the m different parameters. Passing to the case of function space, equation 1 becomes

$$v(x) = f(x; t_1, t_2, \cdots, t_m). \tag{2}$$

The points along a curve in function space are represented by curves of a 1-parameter family, $v(x; t)$. Two-dimensional principal projections of such a curve are obtained by plotting $v(x_1; t)$ and $v(x_2; t)$ as

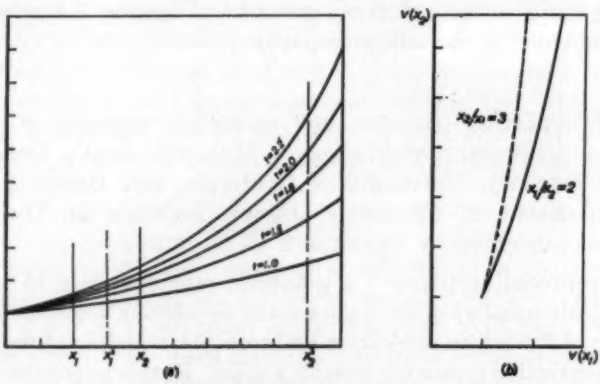

Fig. 1.—Representation and two principal projections of a function space curve.

the two Cartesian coordinates of the projection of a point of the curve. For example, if the equation of the curve is $v(x) = e^{xt}$, the equation of each principal plane projection is of the form $v(x_2) = [v(x_1)]^{(x_2/x_1)}$. In Fig. 1*a* each curve for a particular value of t represents one point on the function space curve. The whole function space curve is represented by a family of curves with different values of t. Each of these points may be projected on the plane whose indices are x_1 and x_2 by the method described in the first paper.[5] Fig. 1*b* shows two principal projections of the curve, one onto the plane x_1x_2, and the other onto the plane $x_1'x_2'$. They were obtained graphically from Fig. 1*a*, and are seen to be members of a parabolic family.

A 3-dimensional principal projection of the curve is obtained in the same manner, using three values $v(x_1; t)$, $v(x_2; t)$, $v(x_3; t)$ as coordinates. It would appear as a space curve, each of whose three principal plane projections is one of the family of principal plane projections of the function space curve.

[5] RANDALL and LONGTIN. *Op. cit.*

The points on a function space curved surface are represented by curves of a 2-parameter family, $v(x; t_1, t_2)$. An example is the representation of a plane, which was discussed in the first paper.[5] Each principal 3-dimensional projection of such a surface is obtained (Fig. 2) by plotting the points $[v(x_1; t_1, t_2), v(x_2; t_1, t_2), v(x_3; t_1, t_2)]$. In general, since two parameters are involved, the resulting projection is a curved surface in a 3-space. The principal plane projections are obtained by plotting only two of the three coordinates and are therefore principal projections of the curved surfaces.

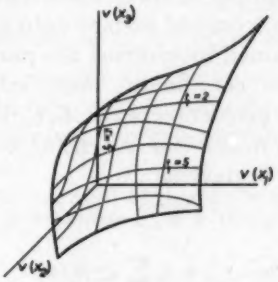

Fig. 2.—A principal projection of a function space curved surface.

The points of a curved 3-space are represented by a 3-parameter family of curves in the function space diagram. Each principal projection onto a 3-space is a 1-parameter family of surfaces $[v(x_1; t_1, t_2, t_3), v(x_2; t_1, t_2, t_3), v(x_3; t_1, t_2, t_3)]$. Each surface of the family is a contour of the curved space for which t_3 (or some function of t_1, t_2, and t_3) is constant. The representation of a curved hypersurface of more than three dimensions by means of space projections is difficult. It can only be obtained by plotting contours of the figure, analogous to the representation of a 4-dimensional figure on a plane by means of 2-dimensional contours of the figure.

Views other than the principal projections may be obtained by rotation of axes. Each of the functions $v(x; t_1, t_2, \cdots, t_m)$ corresponding to particular values of $t_1, t_2, \cdots, t_m$) is expressed in terms of the rotated axis system by Fourier expansion, and then a series of principal projections is taken.

SURFACES LYING IN A HYPERPLANE

If the curved hypersurface is limited to an oblique plane hyperspace, its equation will be of the form

$$\begin{aligned} v(x; t_1, t_2, \cdots, t_m) &= v_0(x) + t_1\epsilon_1(x) + t_2\epsilon_2(x) + \cdots + t_m\epsilon_m(x) \\ f_1(t_1, t_2, \cdots, t_m) &= 0 \\ f_2(t_1, t_2, \cdots, t_m) &= 0 \\ &\cdots\cdots\cdots \\ f_k(t_1, t_2, \cdots, t_m) &= 0, \end{aligned} \tag{3}$$

where the functions $\epsilon_i(x)$ are orthonormal and lie in the particular hyperspace in which the curved surface lies. Since there are only $(m-k)$ independent parameters, the curved surface has $(m-k)$ dimensions, and lies entirely in an m-dimensional space.

A projection of such a curved surface onto a space parallel to that in which it lies[5] is obtained by plotting the parameters $t_1, t_2, \cdots, t_m$, as coordinates.[6] These coordinates must satisfy the k equations $f_i(t_1, t_2, \cdots, t_m) = 0$. A projection of $v(x; t_1, t_2, \cdots, t_m)$ onto the space of $E_1(x), E_2(x), \cdots, E_m(x)$ (the set $E_i(x)$ being orthonormal, but oblique to the set $\epsilon_i(x)$ is given as

$$\begin{aligned} v_E(x; t_1, t_2, \cdots, t_m) &= v_{0E}(x) + t_1 \sum_j \epsilon_{1j}E_j(x) + t_2 \sum_j \epsilon_{2j}E_j(x) \\ &\quad + \cdots + t_m \sum_j \epsilon_{mj}E_j(x) \\ &= v_{0E}(x) + \sum_j (t_1\epsilon_{1j} + t_2\epsilon_{2j} + \cdots + t_m\epsilon_{mj})E_j(x), \end{aligned} \tag{4}$$

in which $v_{0E}(x)$ is considered as the Fourier expansion of $v_0(x)$ in terms of the set $E_i(x)$ and ϵ_{ij} is the Fourier coefficient of $E_j(x)$ in the expansion of $\epsilon_i(x)$. The projection of the curved surface is found by plotting the m coefficients $s_j = (t_1\epsilon_{1j} + t_2\epsilon_{2j} + t_3\epsilon_{3j} + \cdots + t_m\epsilon_{mj})$ as m Cartesian coordinates,[6] while requiring that the parameters $t_1, t_2, \cdots, t_m$ satisfy equations 3. Since the coefficients ϵ_{ij} are constants depending on the relative direction of the original and the projection space, the coordinates in the projection are simply linear combinations of the parameters t_i.

HYPERSPHERE LIMITED TO AN m-SPACE

If the surface considered is a hypersphere of $(m-1)$ dimensions, then $k = 1$, and the single equation restricting the parameters is

$$t_1^2 + t_2^2 + \cdots + t_m^2 = r^2, \tag{5}$$

r being the radius of the hypersphere. From the theory of bilinear forms it is found that if the functions $E_j(x)$ are chosen to give the

[6] This operation implies that the origin in the projection plane is chosen at a point which represents the projection of $v_0(x)$.

proper orientation of the vectors $\mathbf{E}_j$ in the projection space, the coordinates $s_j = \sum_i t_i \epsilon_{ij}$ must satisfy an equation of the form

$$\sum_j (a_j s_j)^2 = r^2 \tag{6}$$

in which the coefficients a_j depend on the angle between the projection space and the space of the sphere. Equation 6 shows that the projected figure is an m-dimensional ellipsoid (or $(m-l)$-dimensional if l of the vectors ϵ_i are orthogonal to the projection plane: this gives an l-edgewise view of the sphere). The orientation of the vectors $\mathbf{E}_i$ is chosen to coincide with the principal axes of the ellipsoid.

POLYNOMIALS IN FUNCTION SPACE

In spaces of a finite number of dimensions the simplest analytic $(n-1)$ dimensional figures are those whose equations are of the form $P(v_1, v_2, \cdots, v_n) = 0$, the function P being a polynomial in the n coordinates $v_1, v_2, \cdots, v_n$.

The homogeneous polynomial of degree m in the n variables may be expressed as

$$P_m(v_1, v_2, \cdots, v_n) = \sum_{i,j,\cdots,p} (v_i v_j \cdots v_p) a_{i,j,\cdots,p} \tag{7}$$

the multiple summation being extended over m indices. If each of the indices covers all values n, each of the combinations $(v_i v_j \cdots v_p)$ will occur $\lfloor n$ times, once for each permutation in which the m indices may appear in the product.

If the coordinates $v_1, v_2, \cdots, v_n$ are components of the vector $\mathbf{v}$ expressed in terms of the orthonormal base vector system, then each of them must be expressed as $v_i'(dx_i)^{1/2}$ in terms of the reduced base vector system. In order to pass from the finite case to function space, it is necessary to assume that each $a_{ij\cdots p}$ is equal to $a'_{ij\cdots p}\,(dx_i\,dx_j \cdots dx_p)^{1/2}$. Then in the limit, the homogeneous polynomial becomes

$$P_m\,|\,[v(x)]\,| = \int_{\Delta}^{(m)} a(x_i, x_j, \cdots, x_p)' v(x_i)' v(x_j)' \cdots v(x_p)' dx_i dx_j \cdots dx_p. \tag{8}$$

Since each product $[v(x_i)'v(x_j)' \cdots v(x_p)']$ corresponding to a particular set of values of $(x_i, x_j, \cdots, x_p)$ may appear several times, not all sets of functions $a(x_i, x_j, \cdots, x_p)$ will generate distinct polynomials.

The homogeneous polynomial of equation 8 may take certain special forms. If $a(x_i, x_j, \cdots, x_p)$ has the value $1/(dx_i dx_j \cdots dx_{p-1})$ when $x_i = x_j = \cdots = x_p$, and zero for all others sets of values of $(x_i, x_j, \cdots, x_p)$, then

$$P_m \mid [v(x)] \mid = \int_a^{a+\Delta} a(x)'[v(x)]^m dx. \tag{9}$$

When $a(x_i, x_j, \cdots, x_p)$ has other less severe singularities, the polynomial may reduce to the form

$$P_m \mid [v(x)] \mid = \int_\Delta^{(k)} a(x_i, x_j, \cdots, x_p)[v(x_i)]^b[v(x_j)]^c \cdots [v(x_p)]^g \, dx_i dx_j \cdots dx_p \tag{10}$$

where k is less than m, and $(b+c+\cdots+g)$ is equal to m.

The general mth order polynomial is expressed as

$$\overset{m}{P} \mid [v(x)] \mid = \sum_{i=0}^{m} P_i \mid [v(x)] \mid, \tag{11}$$

the term for $i=0$ being a constant. The equation $\overset{m}{P} \mid [v(x)] \mid = 0$ then represents a general type of hypersurface analogous to the ordinary case $P(v_1, v_2, \cdots, v_n) = 0$. The most general equation of a hypersurface in function space is

$$F \mid [v(x)] \mid = 0, \tag{12}$$

where F is any functional whatever. This corresponds to the ordinary case $f(v_1, v_2, \cdots, v_n) = 0$.

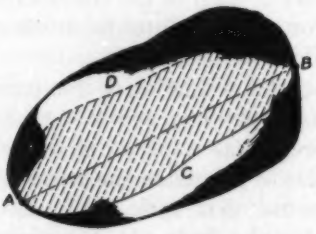

Fig. 3.—Sections of a 3-dimensional solid.

PLANE AND SOLID SECTIONS OF A HYPERSURFACE

In the descriptive geometry of 3-space it is necessary to represent a curved surface by means of contours, which are parallel plane sections of the solid figure. Some idea of the n-dimensional figure may be obtained in a similar manner by projection of two 3-dimensional sections of the figure onto 2- and 3-spaces.

In so doing, it must be remembered that in the 3-dimensional case a plane cuts the surface in a curve (curve $ACBD$ in Fig. 3), while a straight line cuts it only in one or more isolated points (A and B). If

the surface is closed, the curve more or less surrounds the surface while the points do not. Furthermore, if the directions of the line and plane are fixed, the plane may be located by fixing one parameter while to locate the line requires the fixing of two parameters. In function space the 2- and 3-dimensional sections are analogous to the linear rather than the plane section of Fig. 3.

The general solid section of the figure represented by equation 12 is obtained when the function $v(x)$ lies in a particular 3-space,

$$v(x) = v_0(x) + t_1\epsilon_1(x) + t_2\epsilon_2(x) + t_3\epsilon_3(x), \tag{13}$$

where t_1, t_2, and t_3 are parameters independent of x and $\epsilon_1(x)$, $\epsilon_2(x)$, $\epsilon_3(x)$ are orthogonal functions lying in the chosen 3-space. The equation of the section is therefore

$$F\,|\,[\{v_0(x) + t_1\epsilon_1(x) + t_2\epsilon_2(x) + t_3\epsilon_3(x)\}]\,| = 0. \tag{14}$$

When the figure is a "polynomial" surface, the equation of a solid section becomes fairly simple. When the function $v(x)$ lies in the space defined by equation 13, the homogeneous polynomials become

$$P_m\,|\,[\{v_0(x) + t_1\epsilon_1(x) + t_2\epsilon_2(x) + t_3\epsilon_3(x)\}]\,|$$

$$= \sum (t_1^b t_2^c t_3^d) \int_\Delta^{(m)} a(x_i, x_j, \cdots, x_p)' \tag{15}$$

$$[v_0(x)]^{(g)}[\epsilon_1(x)]^{(b)}[\epsilon_2(x)]^{(c)}[\epsilon_3(x)]^{(d)}dx_i dx_j \cdots dx_p$$

where the brackets $[v_0(x)]^g$ etc. represent the products of g factors of the form $v_0(x_i)$ etc., and the sum $(b+c+d+g)$ is equal to m. Hence the general polynomial $\bar{P}\,|\,[v(x)]\,|$ becomes a general polynomial in the parameters t_1, t_2, and t_3 when $v(x)$ lies in the given 3-space. The constant coefficients in this polynomial are sums of integrals of the form which appears in equation 15.

The solid sections of a figure by the 3-space of equation 13 is to be found by plotting the parameters t_1, t_2 and t_3 as Cartesian coordinates. Thus the solid sections of a polynomial hypersurface of degree m are found to be "polynomial" solids of degree equal at most to m. That is, the equations of the sections are of the form $P(t_1, t_2, t_3) = 0$, where P is a polynomial of degree equal at most to m.

HYPERSPHERE IN FUNCTION SPACE

The vector $\mathbf{v}$ defines a point in the hypersphere of radius R, if its length is constant and equal to R. Hence the equation of the hypersphere is

$$\int_\Delta [v(x)]^2 dx = R^2. \tag{16}$$

Taking a section by the plane of equation 13, we find

$$t_1^2 + t_2^2 + t_3^2 + |\mathbf{v}_0|^2 = R^2 \tag{17}$$

provided $v_0(x)$ is taken orthogonal to $\epsilon_1(x)$, $\epsilon_2(x)$, and $\epsilon_3(x)$ (which is always possible).

Equation 17 is the equation of a sphere of radius $(R^2 - |\mathbf{v}_0|^2)^{1/2}$, $|\mathbf{v}_0|^2$ being the distance from the cutting 3-space to the center of the sphere.

If these successive sections (corresponding to a series of values of $\mathbf{v}_0 = p\hat{\mathbf{v}}_0$ in which only a single parameter, p, is varied) are all projected on a space parallel to the cutting spaces, they will appear as a series of concentric spheres of which the largest has the radius R. If instead the projection is taken onto a space oblique to the cutting spaces, the sections will appear as a series of similar ellipsoids (cf. equation 6) whose centers lie at points which are the projections of $\mathbf{v}_0$.

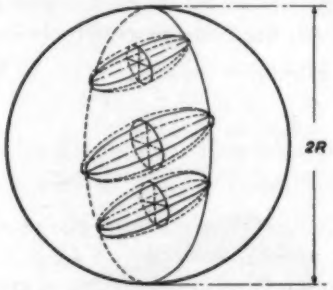

Fig. 4.—Projected sections of a hypersphere.

A series of such sections is shown in Fig. 4. They are each shown as twice tangent to a sphere of radius $2R$ (a view of the great sphere which is parallel to the projection space), the locus of the points of tangency being a great circle of the sphere. This is an intuitive generalization of the analogous case in which circular sections of a sphere appear in two dimensions as ellipses tangent to a circle of radius $2R$. The proof would result from an application of the theory of bilinear forms. Different choices of the vector $\hat{\mathbf{v}}_0$ would give other than great circle loci of the points of tangency. Particular directions of the projection space might cause the ellipsoid to become tangent to the great-sphere in a small (or great) circle.

PROJECTED DENSITIES

Imagine a nonrefractive, nonreflecting translucent sphere. This sphere appears in a single view as a circular region, which is densest

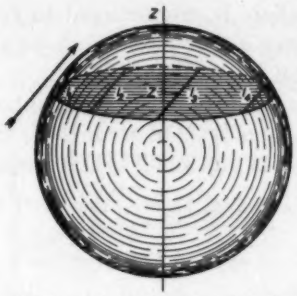

Fig. 5.—Illustration of significance of projected density.

near the center and quite attenuated at the circumference. The apparent density at each point is proportional to the length of linear segment of the sphere, of which the point is an end-on view. For example, in Fig. 5 the segments l_1, l_2, l_3, and l_4 are parallel to the projection rays. Each appears as a point that has a density proportional to its length. This is the projected density of the sphere at this point.

If the projection is taken onto the axis Z rather than onto a plane, all the points in a plane normal to Z appear in the single point Z_1, of density proportional to the area of a plane section of the sphere. This is the projected density of the sphere in terms of a line or 1-dimensional-projection.

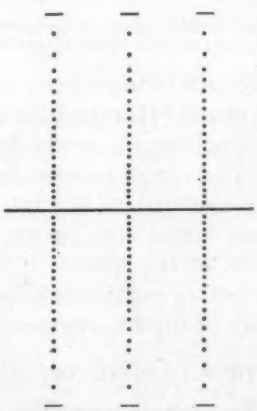

Fig. 6.—Density projections of 3-dimensional sphere on 3-principal axes.

By equation 17, the $(n-1)$ dimensional section of a hypersphere by a space which is distant $|\mathbf{v}_0|$ from the center of the sphere has a radius

$$r = (R^2 - |\mathbf{v}_0|^2)^{1/2}. \tag{18}$$

The volume of this sphere is proportional to $r^{(n-1)}$. Levy[7] has shown that this volume becomes either zero or infinite, depending on whether r is less or greater than $[(n-1)/2\pi e]^{1/2}$.

The largest of these sections is the great sphere whose radius is R, corresponding to a value of $|\mathbf{v}_0|^2$ of zero. If V_0 and V are the volumes of the great sphere, and of any small sphere respectively, then

$$V/V_0 = \lim_{n\to\infty} \left[1 - (|\mathbf{v}_0|/R)^2\right]^{\frac{n-1}{2}} = \exp\left[-(|\mathbf{v}_0|/R)^2(n-1)/2\right] \tag{19}$$

This ratio is greater than zero only if $|\mathbf{v}_0|$ is of the order of $R/(n-1)^{1/2}$.

In any projection of the hypersphere onto a straight line, the projected density is infinitely greater at the center than at any other point. It decreases exponentially with the distance from the center, and becomes almost zero at an infinitesimal distance from the center. It becomes exactly zero at a distance of R from the center.

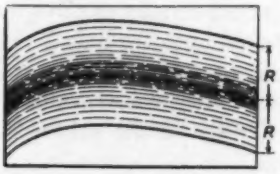

Fig. 7.—Projected density of an n-dimensional hypersphere in the function space diagram.

Fig. 7 shows the projections of the density of an n-sphere onto each of the principal axes, arranged to form a function space diagram. The density decrease in receding from the center is shown less abrupt than the actual case, for the purpose of representation. This density distribution may also be considered as the result which would be obtained by superposing all curves $v(x)$ having lengths less than R as measured from the center of the sphere. It is a composite function space diagram of all vectors which determine points within the sphere, and, as such, may be used to represent the sphere.

OTHER ANALYTIC FIGURES

Other n-dimensional figures may be studied in the same manner, by means of sections and projected densities. For example, the hyperellipsoid whose equation is

$$\int_\Delta [v(x)/a(x)]^2 dx = 1 \tag{20}$$

[7] LEVY, P. *Op. cit.*

has principal axes equal to $a(x)$. All its representations may be obtained from those of the sphere by magnifying the various axes in the proportions $a(x):R$. The projected density diagram is shown in Fig. 8.

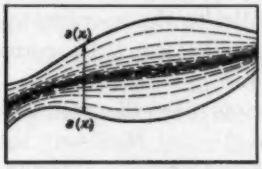

Fig. 8.—Projected density of an n-dimensional hyperellipsoid in the function space diagram.

Of all the sections of a function-space figure, the most interesting is the section that appears greatest in any particular projection. This corresponds to the outline in a 2-dimensional view of a solid figure and is represented by the great-sphere in the case already discussed. In particular cases it may be found by analytic or intuitive methods. In general it is found by trial, from the construction of a large number of sections.

RECTANGULAR HYPERPARALLELOPIPED

If we interpret the vector equation

$$(\mathbf{h} + \mathbf{l}) \geqq \mathbf{v} \geqq \mathbf{h} \tag{21}$$

to mean that each of the components v_i lies between the limits h_i and (h_i+l_i) and may be equal to either limit independent of whether any other component lies at its limit, then the vector $\mathbf{v}$ traverses all points interior to (and on the surface of) a rectangular parallelopiped. If v_i is

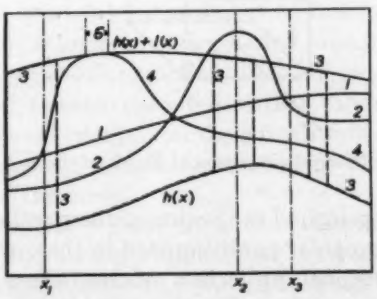

Fig. 9.—Function space diagram of a rectangular hyperparallelopiped.

equal to h_i, and none of the other components lies at either of its limits, the vector **v** traverses a limited rectangular portion of an $(n-1)$ dimensional hyperplane—one of the faces of the parallelopiped. When v_i is equal to (h_i+l_i), **v** traverses the opposite face. Hence the "reduced" length of the side normal to these faces is l_i. The parallelopiped has its edges parallel to the coordinate axes. They are respectively equal to the components of **l**. Its corner which is nearest the origin lies at the end of **h**.

Fig. 9 shows the function space diagram for a hyperparallelopiped. The curves $h(x)$ and $h(x)+l(x)$ represent the vectors **h** and **h**+**l**. Curve 1 represents a point entirely interior to the parallelopiped. Over a portion of the interval Δ, curve 2 passes outside the limit of $h(x)+l(x)$, and hence represents a vector which does not satisfy equation 21. It represents a point outside the parallelopiped. Curve 3 represents a function all of whose values are equal to one or the other of the limits. Hence it represents a vertex of the parallelopiped. The curves $h(x)$ and $[h(x)+l(x)]$ represent two opposite vertices. Curve 4 has $(n\delta/\Delta)$ of its components equal to their respective upper limits. It represents a point which lies in a $(1-n)\,\delta/\Delta$-dimensional face of the parallelopiped.

If the function $l(x)$ is constant independent of x, the vector l being equal to $l\mathbf{e'}_{a^{a+\Delta}}$, the parallelopiped becomes a hypercube. Hence the hypercube is represented by curves, $v(x)$ which lie entirely within the region bounded by two curves, $h(x)$ and $[1+h(x)]$, which are vertically equidistant for all values of x.

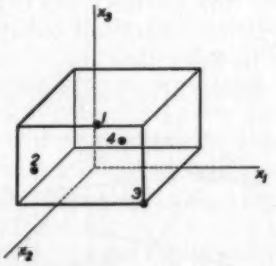

Fig. 10.—Principal projection of Fig. 9 on the x_1–x_2–x_3-space.

Fig. 10 shows a principal projection of the parallelopiped of Fig. 9. It is seen as a rectangular parallelopiped in three dimensions. In any principal m-dimensional projection of the figure, the coordinates must each satisfy an inequality $(h_i+l_i) \geqq v_i \geqq h_i$, and hence all the

projected points must lie inside a rectangular parallelopiped. The projection appears as this parallelopiped.

Oblique views and sections of the parallelopiped may be obtained in the manner already described for analytic surfaces. A consideration of the spheres inscribed and circumscribed in a hypercube will indicate the difficulties involved. The radius of the inscribed sphere has a length equal to $\frac{1}{2}l(\Delta/n)^{1/2}$ in terms of the unit base vector system (the length of a side of the cube is $l(\Delta/n)^{1/2}$ in terms of this system). The radius of the circumscribed sphere is half the length of the long diagonal, which is $l|\mathbf{e}'_{a^{n+\Delta}}| = l$. If the circumscribed sphere is of finite radius, the inscribed sphere has an infinitesimal radius.

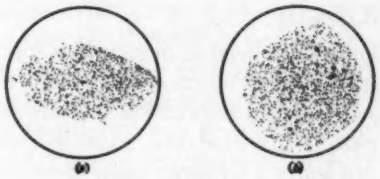

Fig. 11.—Projections of the vertices of a hypercube.

The cube has 2^n vertices which must lie in the surface of the circumscribed hypersphere. In the projection they will appear scattered irregularly throughout the interior of the bounding great-sphere, the distribution depending on the orientation of the projection space. No two vertices lying on the same edge may appear in the projection at a distance greater than $l(\Delta/n)^{1/2}$ (i.e., the length of the edge on which they lie), which is infinitesimal. Hence the distribution of vertices will be macroscopically dense in certain regions of the projection. If the projection is edgewise to a number of dimensions of the hypercube, the region may be limited by a surface which is tangent to the projection of the inscribed sphere [the greatest breadth observed in the projection along the direction normal to the edgewise faces is equal to the length of a side]. In other cases the vertices will more nearly appear to fill the great-sphere boundary of the circumscribed sphere. Fig. 11*a* shows a conceivable nearly edgewise view, while Fig. 11*b* is less nearly edgewise to any of the faces.

In the special case of a finite number of dimensions, the various oblique views are more simply described. The number of vertices is finite, while the edges appear to have finite rather than infinitesimal lengths. The resulting figures are common in treatises on polytopes.

SUMMARY

Regions of function space having one dimension (curved line) and two dimensions (curved surface) are easily represented in the function-space diagram by a family of curves having one or two parameters, respectively. In any 3-space projection they appear as a curved line or curved surface.

Any figure having more than three dimensions is of course difficult to represent in a space of three dimensions. The problem is like that of representing a solid figure on paper. Three methods have been illustrated, namely:

1. The projected outline of the figure.
2. The projected sections or contours.
3. The projected density.

A fourth method commonly used in descriptive solid geometry is that of the illuminated and shaded surface. While this method often gives the most clearly readable representation of solid figures, its application to function space is questionable, since the laws of illumination and reflection are not known for more than three dimensions.

ZOOLOGY.—*A review of the subspecies of the indigo snake* (Drymarchon corais).[1] HOBART M. SMITH, Smithsonian Institution. (Communicated by HERBERT FRIEDMANN.)

In the most recent study of *Drymarchon* (Amaral, Mem. Inst. Butantan **4**: 323–330, 1929), three subspecies of the monotypic genus are recognized: *corais corais*, *corais melanurus*, and *corais couperi*. The last named is stated to range "from northeastern Mexico to southeastern United States." As has been shown by Blanchard (Papers Michigan Acad. Sci., Arts and Lett. **4**: 28, 1925), and accepted by Stejneger and Barbour (Check List N. Amer. Amph. Rept., ed. 4, pp. 106–107, 1939), the form in Florida and Georgia possesses characters in both coloration and scutellation that differentiate it from any other population of the genus; and to this form must be applied the name *couperi*, with type locality in Georgia. Present records further demonstrate that there is a hiatus between the range of *couperi* and that of the *Drymarchon* of Texas, this hiatus occurring in the region of Louisiana, eastern Texas, and Mississippi.

Amaral (*op. cit.*) indicates that the area of intergradation between his composite *couperi* and his *melanurus* of Central America and central Mexico may occur in the region of Tamaulipas and Veracruz. Since it can be demonstrated that the southwestern Texas form of

[1] Received April 10, 1941.

Drymarchon is not *couperi*, the identity of the forms that are inferred to intergrade in Mexico is left in doubt.

This confusion has led to a reexamination of specimens in the U. S. National Museum and in the EHT-HMS collection and to an attempt to redefine the various forms of the genus. In the United States and South America the problem seems relatively simple, as only two well-defined forms in each area are represented by specimens examined. In Mexico and northern Central America, however, the problem becomes complicated. Five of the seven recognizable forms occur in this area. Lack of adequate material of certain subspecies has hampered a ready understanding of the variation and distribution of all forms. Most difficult to handle of all are the young, which are frequently unidentifiable. With more material, accompanied by specific locality data, probably the difficulties encountered in separating the young may be eliminated. The young of three forms are definitely identifiable, through their peculiar scutellation or coloration, or both. Those of the other four forms can be separated into two groups, but association with either one of the two subspecies in each group is now too vague to be reliable—other than by geographic probability.

I am indebted to Dr. E. H. Taylor for his suggestions and loan of material during the course of this study, which was begun some time ago at the University of Kansas. An important portion of the material utilized was collected and studied during my tenure of the Walter Rathbone Bacon Traveling Scholarship of the Smithsonian Institution.

KEY TO THE FORMS OF DRYMARCHON

1. Belly and tail light throughout their length; no *distinctive* dark marks on edges of subocular labials; in adults, anterior portion of body darker than posterior portion and tail ..... *corais corais*
   Tail and at least posterior part of belly usually dark (black); if not, distinctive dark marks present on edges of at least subocular labials ... 2
2. Antepenultimate labial separated from temporals by contact of adjacent supralabials; all black except chin and sometimes a few areas on supralabials; caudals less than 68; ventrals 185 to 189 in males, 193 to 195 in females ..... *corais couperi*
   Antepenultimate labial in contact with temporals or lower preocular, or both 3
3. Subcaudals less than 68 (55 to 65); ventrals 193 or less; scale rows usually 14 near anus ..... *corais erebennus*
   Subcaudals more than 68 (69 to 83); scale rows usually 15 near anus 4
4. Anterior portion of body light brown, extreme posterior portion and tail black; three vertical black streaks on posterior edges of subocular labials, and one on posterior edge of seventh labial, never any on preocular labials (either above or below); lateral gular scales never black-tipped; young lighter anteriorly than posteriorly, like adults, but with very broad, light, chevron-shaped bands covering two scale lengths .... *corais melanocercus*

Entire body and tail light brown above, or all black; light bands in young specimens narrow, covering about one scale length (?).....5

5. Entire body brown above, and no darker posteriorly than anteriorly; ventral surface of tail and posterior portion of body dark, but not black; young (and some adults) with distinct, longitudinal, short black streaks on anterior part of body.....*corais unicolor*

Entire body nearly uniform black above; belly black on posterior portion, subcaudal surface black.....6

6. Light areas on supralabial region white or cream, very sharply defined from the black borders; anterior portion of belly mostly light, salmon pink in color.....*corais rubidus*

Most of head, including sides, black; most of belly black, the light portions cream or white, not reddish.....*corais orizabensis*

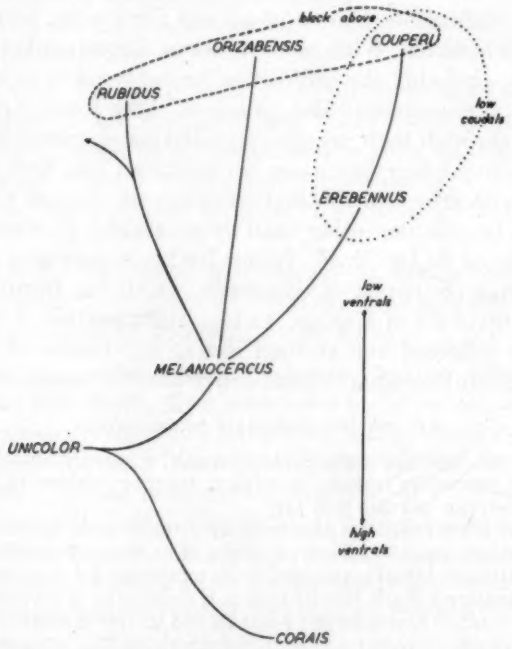

Fig. 1.—Possible phylogeny of the subspecies of *Drymarchon corais*.

Evolution within the genus may be traced by the general trend toward melanism in end forms, as in *couperi*, *rubidus*, and *orizabensis*. Accordingly a form that is the least melanistic is indicated as the more primitive; this form is *unicolor*. The geographically centralized position of *unicolor* in relation to others supports the premise that it is the most primitive. Evolution has proceeded in two directions from this common ancestor, both geographically and in pattern. In one direc-

tion, toward the south, evolved *corais*, now restricted to South America. This branch exemplifies a different trend in pigmentation than does the other branch—progression of melanism from the cephalic region toward the tail. The trend in the second branch is from the tail toward the head. In both branches pattern evolution is directed toward an end form completely black in color.

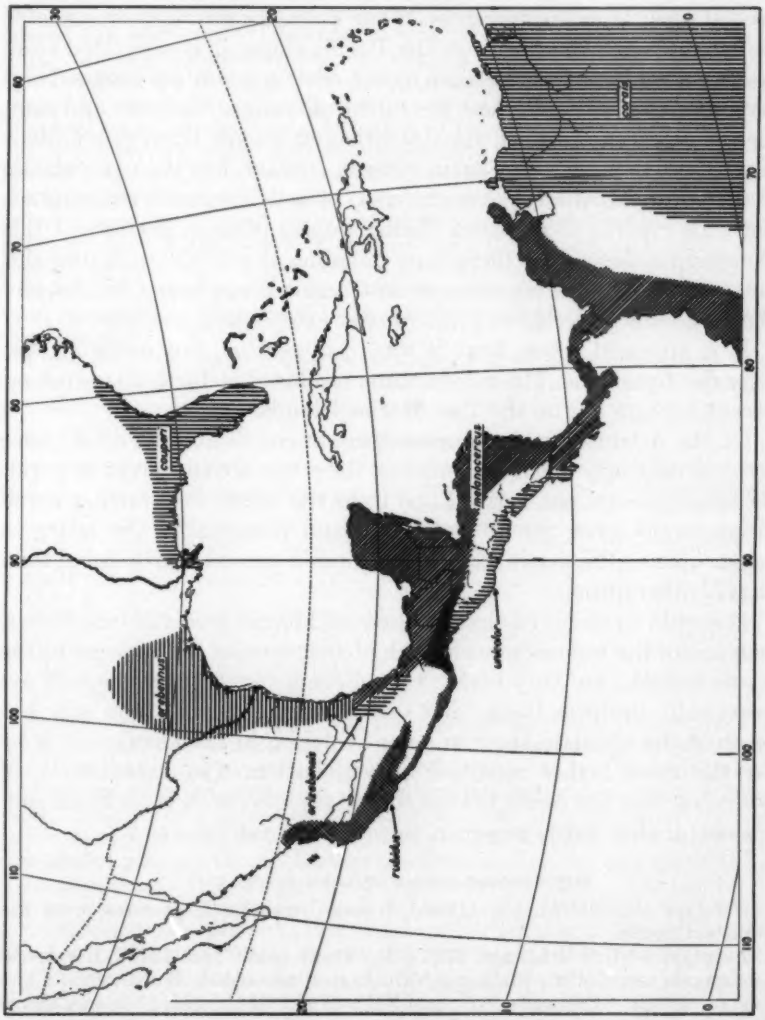

Fig. 2.—Distribution of the subspecies of *Drymarchon corais*. Base map courtesy McKnight and McKnight.

The fact that *unicolor* is now widely separated from *corais* by *melanocercus* in Costa Rica, Panama, and northern South America does not prove the former could not have given rise to *corais*. It is very unlikely that, once the tail-head tendency of pattern change was established in *melanocercus*, it should be reversed to produce the characters now shown by *corais*.

Development of other forms in the genus appears to have proceeded solely from *melanocercus*. While *unicolor* extends a considerable distance toward the north on the Pacific slope, it is separated from *melanocercus* the whole distance by the central mountain ranges. Near the Isthmus, however, where the mountain ranges are lower and complete connection between the Atlantic and Pacific coast populations is possible, the two forms again come in contact, but the more plastic of the two (*melanocercus*) has changed, as in this region it is intergrading with *rubidus* of northern Pacific slopes; perhaps because of this change in *melanocercus* there is no mingling of *unicolor* with it in this area; the two live in the same general region in southern Chiapas, and the ranges may overlap to a still greater extent than now known.

It is apparent, then, that it was *melanocercus*, not *unicolor*, that gave rise to *rubidus*. The *rubidus* stem produced no further subspecies, except perhaps one on the Tres Marias Islands.

On the Atlantic coast *melanocercus* gave rise to another color phase (*orizabensis*) very much like *rubidus;* these two are conceived as parallel developments not derived one from the other. Still farther north *melanocercus* gave rise to *erebennus;* and presumably the latter to *couperi*, since these two hold in common a caudal count lower than that of other forms.

It should be observed that all three end forms (*rubidus, orizabensis, couperi*) of the *melanocercus* branch of *Drymarchon* (as opposed to the *corais* branch) are very black; two of them (*orizabensis, couperi*) are practically uniform black; and one of them (*couperi*) not only has reached the ultimate stage in color evolution in the genus, but is by far the most highly modified in scutellation. The expectation, of course, is that the *corais* branch should possess one or more black subspecies; if they exist, however, they are not yet known.

Drymarchon corais unicolor subsp. nov.

Holotype.—U.S.N.M. no. 110865, female, from La Esperanza, near Escuintla, Chiapas.

Paratypes.—U.S.N.M. nos. 6757A-B, "Guatemala"; no. 12687, Escuintla, Guatemala; no. 79960, Managua, Nicaragua; no. 46464, Huehuetan, Chiapas; no. 30424, "Tehuantepec"; and EHT-HMS (HMS 14556) from Colonia Hidalgo, 8 kilometers north of La Esperanza, Chiapas.

Diagnosis.—Adults uniform light brown above, posterior portion no or little darker than anterior, sometimes longitudinal black streaks anteriorly; venter light, becoming somewhat darker posteriorly and under tail, but not black; young with short, black streaks anteriorly, posteriorly with narrow, irregular, light crossbars. Ventrals 192 to 206; caudals 70 to 77 (females); totals 266 to 281 (females). Antepenultimate labial in contact with temporals of postoculars, or both; scale rows posteriorly usually 15.

Description of holotype.—Head scales normal; supralabials eight, the sixth in contact with lower anterior temporal; infralabials nine, first five in contact with chin shields, four in contact with anterior chin shields; one preocular, two postoculars; temporals in two rows, three in lower row, two in upper; lower posterior temporal narrowly in contact with parietal on one side (between the two upper temporals), narrowly separated on the other; posterior chin shields distinctly shorter and smaller than anterior; ventrals 195; anal entire; caudals 71. Total length 1570 mm; tail 320 mm.

Dorsal surface of entire body and tail uniform light brown, with the exception of irregular, short, poorly defined, diagonal black streaks on anterior portion of body; a black, diagonal patch on nape, poorly defined and short. Sides of head light brown, as dorsal surface; a vertical black mark on the posterior edge of the fourth to the seventh supralabials, and on the corresponding infralabials; posterolateral gular scales darker at their tips.

Belly light anteriorly, posterior fifth becoming brown, as subcaudal surface; no portion of belly or tail black, save a very few marks on the edges of some ventrals.

Variation.—The paratype series compares well with the holotype in coloration. In one the dark streaks are more prominent. In none is the posterior portion of the belly, or the subcaudal surface, black.

TABLE 1.—SCALE COUNTS IN UNICOLOR

Number	Sex	Ventrals	Caudals	Scale rows	Supralabials	Antepenultimate labial
6757	♂	206	68+	17–15	8–8	Contact
6757	♀	204	77	17–15	8–9	Contact
30424	♀	192	75	17–15	8–8	Contact
12687	♀	199	71	17–15	8–8	Contact
46464	♀	200	70	17–15	8–8	Contact
79960	♀	204	75	17–15	8–8	Contact
110865	♀	195	71	17–15	8–8	Contact
14556	♀	200	52+	17–15	8–8	Contact

Remarks.—Almost certainly this form intergrades with *melanocercus* in southern Nicaragua or northern Costa Rica. The Managua, Nicaragua, paratype is fairly typical, however. North of Nicaragua the two forms do not intergrade, as they are separated by continuous, high ranges of mountains except toward the Isthmus of Tehuantepec. Here they do not intergrade, either, as typical *unicolor* occurs at La Esperanza, Chiapas, with *melanocercus-rubidus* intergrades. An ecological segregation of the two types at La Esperanza is indicated. The single intergrade secured there (No. 110874) as well as two intergrades from Tonalá, Chiapas (Nos. 110875–6) were found in the forested hills, while the two *unicolor* collected near La Esperanza were found on the coastal plain. Presumably the latter subspecies occurs still farther north in the same habitat. Unfortunately no specimens are known from the coastal plain between the vicinity of Tehuantepec and La Esperanza.

The *rubidus-melanocercus* intergrades are further discussed in the description of the former subspecies.

Drymarchon corais corais (Boie)

Coluber corais Boie, Isis, 1827, p. 537; Schlegel, Essai Phys. Serp. **2**: 139–141, pl. 5, figs. 9, 10. 1837.

Geoptyas flaviventris Steindachner, Sitzb. Akad. Wiss. Wien **55**: 271, pl. 4, figs. 4–7. 1867 (Matogrosso, Cuyaba und dem Rio Vaupe).

Spilotes corais suborbitalis Peters, Monatsb. Preuss. Akad. Wiss., Berlin, 1868: 641 (Caracas, Venezuela).

Spilotes corais xanthurus Brown, Proc. Acad. Nat. Sci. Philadelphia, 1893: 433 (type locality unknown; not Veracruz, as suggested).

Drymarchon corais corais Amaral, Mem. Inst. Butantan **4**: 325–327, pl. 1929.[2]

Type locality.—America.

Diagnosis.—Adults dark anteriorly, light posteriorly on back; belly and subcaudal surface white, except edges (lateral); young no darker anteriorly

TABLE 2.—SCALE COUNTS IN CORAIS

Number	Sex	Ventrals	Caudals	Scale rows	Supralabials	Antepenultimate labial
5579	♀	208	72	17–15	8–8	Contact
5579	♀	209	75	17–15	8–8	Contact
11309	♀	210	—	17–15	8–8	Contact
12535	♂	205	83	17–15	8–8	Contact
15233	♂	202	80	17–15	8–8	Contact
60660	♂	—	79	17–15	8–8	Contact
60749	♂	206	82	17–15	8–8	Contact
66871	♀	210	74	17–14	8–8	Contact
84523	♀	205	74	17–15	8–8	Contact

than posteriorly, but with more or less chevron-shaped, broad, light bands, not interrupted and covering about two scale lengths; supraocular labials not distinctively black-edged (see below) in young or adult. Ventrals 190 (?) to 217 (males 190 to 210, females 205 to 217); caudals 72 to 84 (72 to 84 in males, 72 to 78 in females); total counts 272 to 292 (males 272 to 292, females 278 to 291). Antepenultimate labial in contact with temporals or postoculars or both; scale rows posteriorly usually 15.

Range.—"Northern Argentina, Paraguay, Bolivia, tropical Brazil, eastern Ecuador and Peru, the Guianas, Venezuela, Trinidad and Tobago" (Amaral, *loc. cit.*).

Specimens examined.—Ten, all in the National Museum: Nos. 5579A-B, 12535, 15233, Trinidad; nos. 60660, 60749, Santa Ana, Peru; nos. 66871, Moengo, Surinam, Dutch Guiana; no. 84523, Pomeroon, 70 miles from Georgetown, British Guiana; no. 11309, Brazil; no. 100756, Terenos, Matto Grosso, Brasil.

Remarks.—The body coloration of adults of this form is not duplicated in any other subspecies of the genus. Most distinctive is the white belly and

[2] *Phrynonax angulifer* Werner, included by Amaral (*op. cit.*, p. 325) in the synonymy of *corais*, does not seem to belong to this genus. It is said to have 21 scale rows; 224 ventrals; fourth, fifth, and sixth labials in contact with the eye; and the nine median scale rows keeled.

subcaudal surface, combined with a light dorsal surface on tail and posterior part of body. Also very strikingly different from other subspecies is the absence of distinctive dark marks on the posterior edges of the subocular labials. These are very characteristic of other subspecies (unless the whole top and side of head is black), but in *c. corais* are absent, although the edges of all dorsal and lateral head scales may be black; or the whole top of the head may be black, the color extending a little below the eye.

In addition to the data afforded by the 10 National Museum specimens, ventral and caudal counts of 44 others, given by Amaral (*loc. cit.*), have been available for establishing the limits of variation in these two characters.

Drymarchon corais melanocercus nom. nov.

Spilotes melanurus Duméril and Bibron, Erp. Gén. **7**: 224. 1854.

Geoptyas collaris Steindachner, Sitzb. Akad. Wiss. Wien **55**: 271, pl. 3, figs. 4–7 (Brazil). 1867.

Drymarchon corais melanurus Stejneger and Barbour (part), Check List N. Amer. Amph. Rept., ed. **2**: 94. 1923—Amaral, Mem. Inst. Butantan **4**: 325, 330 (part). 1929.

Type locality.—"Mexico."

Diagnosis.—Adults light brown anteriorly, dark (black) on posterior fourth or fifth of body and on tail, both above and below; young generally a little lighter anteriorly than posteriorly, the bands (where visible, usually toward middle of body) similar to those of young *c. corais;* black marks on subocular labials very sharply defined, rest of head very light; no black marks on labials preceding orbit, nor on lateral gular scales; diagonal black mark on each side of neck very well defined. Ventrals 191 to 214 (males 191 to 208, females 197 to 214); caudals 71 to 88 (males 71 to 88, females 71 to 80); totals 262 to 296 (males 272 to 296, females 268 to 279). Antepenultimate labial in contact with temporal or postocular or both; scale rows usually 15 posteriorly.

Range.—Pacific slopes of Peru and Ecuador; northern Colombia; Central America north to northern Veracruz on the Atlantic side, to southern Nicaragua on the Pacific side.

Specimens examined.—Fourteen. One in the EHT-HMS collection (no. 11636) is from Mérida, Yucatán. The remainder, in the National Museum; are from VERACRUZ: Mirador? (no. 25093). CHIAPAS: Palenque (no. 110871); TABASCO: Tenosique (no. 110870). YUCATÁN: Chichen Itza (no. 46393); Yucatán (no. 6554). GUATEMALA (Petén): Pacomon (no. 71371); Piedras Negras (nos. 110872–3). COSTA RICA (no. 61947). PANAMÁ (no. 53629): Washington Station (no. 8393). COLOMBIA: Cayo Papoyal, Bolivar Dist. (no. 54338). ECUADOR (no. 14025).

Remarks.—This subspecies is remarkably well defined and uniform in character of color pattern throughout its entire range from South America to central Mexico. It presumably intergrades with *unicolor* in southern Nicaragua; intergradation elsewhere with it seems impossible (see discussion of latter). Intergradation with *orizabensis, rubidus,* and *erebennus* is actually demonstrated, however, by specimens now available (see discussions of each form).

In addition to the data afforded by the 14 specimens examined, ventral and caudal counts of nine others, given by Amaral (*loc. cit.*), have been available. The ventral, caudal, and total counts of these specimens indicate that two subspecies may be involved, although they do not seem separable on the

basis of color characters. One population is represented by specimens from Mexico and Petén, Guatemala, the other by specimens from Costa Rica south. Unfortunately no material is available from the intermediate area. The counts thus segregated are as follows:

	Northern		Southern	
	Males	Females	Males	Females
Ventrals	191–202 [3]	197–202 [4]	203–208 [8]	204–214 [6]
Caudals	71–80 [2]	71–77 [4]	77–88 [8]	73–80 [5]
Total	262–278 [2]	268–279 [4]	280–296 [8]	279–294 [4]

More specimens will be necessary to demonstrate whether these apparent differences are real. In each area there appears to be a general trend toward higher counts to the south, lower counts to the north.

TABLE 3.—SCALE COUNTS IN MELANOCERCUS

Number	Sex	Ventrals	Caudals	Scale rows	Supra-labials	Antepe-nultimate labial	Locality
25093	♂	191	71	17–15	—	Contact	Veracruz
11636	♂	198	80	17–15	8–8	Contact	Yucatán
6554	♀	197	76+	17–15	8–8	Contact	Yucatán
46393	♀	200	77	17–15	8–8	Contact	Yucatán
110871	♂	202	71+	17–15	8–8	Contact	Chiapas
110870	♀	198	71	17–15	8–8	Contact	Tabasco
110872	?	197	77	17–15	8–8	Contact	Petén
110873	♀	202	71	17–14	8–8	Contact	Petén
71371	♀	199	74	17–15	8–8	Contact	Petén
61947	♂	205	83	17–15	8–8	Contact	Costa Rica
53629	♀	209	80	17–15	8–8	Contact	Panamá
8393	♂	203	83	17–15	8–8	Contact	Panamá
54338	?	—	80	–15	8–8	Contact	Colombia
14025	♀	207	—	17–15	8–8	Contact	Ecuador

The name *Spilotes melanurus* Duméril and Bibron is not available for this subspecies, since it was suppressed by Gray (Cat. Snakes Brit. Mus., 1858, p. 97), who placed in the same genus (*Spilotes*) *Coluber melanurus* Schlegel (1837). Gray recognized *Spilotes melanurus* (Schlegel) and treated Duméril and Bibron's name as a variety ("Var. 1") of *Spilotes corais*. The only other name which has been applied to this subspecies (*Geoptyas collaris* Steindachner) is also suppressed as a secondary homonym of *Coluber collaris* Ménétr., 1832 (=*Contia collaris*), since Boulenger (Cat. Snakes Brit. Mus. 2: 31. 1894.) included Steindachner's name in the synonymy of *Coluber corais* Boie.

Drymarchon corais rubidus subsp. nov.

Holotype.—U.S.N.M. no. 46430, female, from Rosario, Sinaloa, collected by Nelson and Goldman.

Paratypes.—Twenty-one, including U.S.N.M. no. 46588, San Sebastián, Jalisco; no. 24683, Maria Madre Island, Tres Marias Islands; no. 46538, Acapulco, Guerrero; nos. 61948–9, Colima; no. 110877, San Diego, near Tehuacán, Puebla; nos. 30425, 110878–84, vicinity of Tehuantepec, Oaxaca; no. 110885, Ixtepec (San Gerónimo), Oaxaca. EHT-HMS no. 5405, Puente de Ixtla, Morelos; no. 5400, Magdalena, Jalisco; nos. 5331, 5406, El Sabino, Michoacán; no. 5591, Huajintlán, Guerrero; and no. 21514, "Guerrero."

Diagnosis.—Dorsal surface, including top of head, uniformly black in

adults; extreme posterior portion of belly and subcaudal surface black; remainder of belly salmon pink, except for lateral black marks; most of labials black-edged posteriorly, the rest of labial area white or pink, sharply differentiated from the black areas. Ventrals 190 to 203, caudals 69 to 78, totals 262 to 275. Antepenultimate labial in contact with temporal or postocular or both; scale rows posteriorly usually 15.

Description of holotype.—Head scales normal; supralabials eight, the sixth in contact with temporal; infralabials nine, five in contact with chin shields, four with anterior chin shields; latter a little shorter and wider than posterior chin shields; one preocular; two postoculars; temporals 2-2; ventrals 193; anal entire; tail tip missing. Total length 973 mm, tail 151 mm (incomplete).

Nearly uniform black above, a little lighter posteriorly; sides of head, as well as top, black, to below eye; posterior borders of all supralabials black, remainder of labial area white, sharply differentiated from black borders; scales in posterolateral gular area black-tipped. Ventral surface of tail and extreme posterior portion of belly black; remainder of belly light, with a slight reddish tinge, except for a black mark on the posterolateral edge of almost every ventral.

Variation.—There is little variation in coloration in the twenty paratypes. Larger specimens are quite uniform black above (type a little lighter posteriorly). Specimens in life have a distinctly salmon-colored belly.

TABLE 4.—SCALE COUNTS IN RUBIDUS

Number	Sex	Ventrals	Caudals	Scale rows	Supralabials	Antepenultimate labial
5331	♂	198	76	17–15	8–8	Contact
5400	♂	190	72	17–15	8–8	Contact
5405	♀	201	69+	17–15	8–8	Contact
5406	?	—	—	—	—	Contact
5591	♀	194	70	17–15	8–8	Contact
21514	♀	197	—	17–15	8–8	Contact
24683	♂	203	82	17–15	8–8	Contact
30425	♀	194	73	17–15	8–8	Contact
46430	♀	193	—	17–15	8–8	Contact
46538	♂	197	77	17–15	8–8	Contact
46588	♂	191	69+?	17–15	8–8	Contact
61948	♂	190	—	17–15	8–8	Contact
61949	?	198	—	17–14	8–8	Contact
110877	♂	196	73	17–15	8–8	Contact
110878	♂	191	72	17–15	8–8	Contact
110879	♂	197	75	17–15	8–8	Contact
110881	♂	192	76	17–15	8–8	Contact
110880	♀	195	67+	17–15	8–8	Contact
110882	♀	197	74	17–15	8–8	Contact
110885	♂	192	75	17–15	8–8	Contact
110883	♀	195	—	17–14	8–8	Contact
110884	♂	197	78	17–15	8–8	Contact

In scutellation the series is uniform with the exception of the Tres Marias Island specimen, which, like certain other snakes on the same Islands, differs from its mainland relatives by having a higher number of ventrals and caudals. It is a male, with 203 ventrals and 82 (+?) caudals; the highest mainland counts are 201 ventrals in a female (highest male count 198), and 78 caudals in a male. If further specimens from the islands consistently have high counts, they should be recognizable as belonging to a different subspecies.

Remarks.—The uniformly dark dorsal coloration, white or pink labial areas and high caudal count separate this subspecies from all others.

Seven specimens represent intergrades between *rubidus* and *melanocercus* They are from "Tehuantepec" (no. 61959); El Barrio, Oaxaca (no. 30526); Santa Efigenia, Oaxaca (no. 46496); Tonalá, Chiapas (nos. 110875–6); La Esperanza, Chiapas (no. 110874); and Valley of Comitán, Chiapas (no. 46587). Three of these specimens—those from Tonalá and La Esperanza—are adults, and definitely are intermediate in character between *rubidus* and *melanocercus*.

TABLE 5.—SCALE COUNTS IN MELANOCERCUS-RUBIDUS INTERGRADES

Number	Sex	Ventrals	Caudals	Scale rows	Supra-labials	Antepenultimate labial
30526	♀	192	76	17–14	8–8	Contact
46496	♀	196	70	17–15	8–8	Contact
46587	♀	193	—	17–15	8–8	Contact
61959	♂	199	73	17–15	8–8	Contact
110874	♀	202	79	17–15	8–8	Contact
110875	♀	193	73+	17–15	8–8	Contact
110876	♂	193	71	17–15	8–8	Contact

They are distinctly lighter anteriorly than posteriorly (not so light as in *melanocercus*); the tail is jet black; the labial marks are less numerous than in *rubidus*, restricted to the subocular and postocular labials (as in *melanocercus*); the light areas of the lips are dull brown (not white as in *rubidus*); the posterolateral gular scales have slightly darker tips; and the belly is little marked with black anteriorly (as in *melanocercus*). These characters are definitely intermediate between those of *rubidus* and *melanocercus*, and cannot be construed as indicating intergradation between either one of these and *unicolor*. In fact, that such intergradation does not occur is indicated by the existence of *rubidus-melanocercus* intergrades at La Esperanza with typical *unicolor*.

The other four specimens unfortunately are juveniles, and accordingly cannot definitely be assigned to the category in which they are here placed as *rubidus-melanocercus* intergrades. They are tentatively referred to this category because of an apparent combination in them of the characters of the two forms, and because of geographic probability. One of them with indefinite locality ("Tehuantepec") has the tail little darker than the rest of the body, and distinctly mottled and banded; the whole body is a little lighter than in the others. This may be a juvenile *unicolor*, although the distinct lateral black marks on the belly do not so indicate. It furthermore may represent an intergrade between *unicolor* and *rubidus* (*rubidus-melanocercus*), but in view of other evidence that such intergradation does not occur, it is not well to draw conclusions upon the basis of this juvenile in which adult features are not evidenced.

The other three specimens appear to be typical intergrades (as characterized by the adults), with the exception that about half the ventrals have a black lateral streak, as typical of adult *rubidus*. The same marks, however, are indicated in the adult *rubidus-melanocercus* intergrades, although poorly defined. Presumably sharp definition of them is a juvenile characteristic in the intergrades; in typical *rubidus* they are sharply defined in the largest adults as well.

Drymarchon corais orizabensis (Dugès)

Morenoa orizabensis Dugès, Proc. Zool. Soc. London, 1905: 517–518, fig. 77.

Type locality.—Orizaba, Veracruz.

Diagnosis.—Adults entirely black above; most of sides of head black; anterior portion of belly heavily pigmented, less than half anterior third light; remainder of ventral surface black; light areas on belly white or cream, not pink; ventrals 186 to 201, caudals 71 to 78. Antepenultimate labial in contact with temporal or postocular or both (rarely not); scale rows rarely reduced to 14 in front of anus.

Range.—Atlantic slopes from near the Isthmus of Tehuantepec about to Mirador, Veracruz. Perhaps restricted to the foothills.

Specimens examined.—Five typical specimens were examined: the type, in the museum at Guanajuato, Mexico; U.S.N.M. no. 110886 and EHT-HMS nos. 5368, 5592–3, all from Potrero Viejo, Veracruz; and U.S.N.M. no. 24999, Mirador, Veracruz.

Remarks.—The type is a juvenile; its association with the very black adults from the same area is prompted for geographic reasons. The form is most nearly like *rubidus*, from which it differs in having the belly almost entirely black (much as in *couperi*), and the light ventral areas not red but white or cream. Its similarity to *rubidus* does not necessarily mean that it is more closely related to that form than to any other. There is evidence that the two are of independent origin.

TABLE 6.—SCALE COUNTS IN ORIZABENSIS

Number	Sex	Ventrals	Caudals	Scale rows	Supra-labials	Antepenultimate labial
5368	♀	201	71	17–15	8–8	Contact
5592	♂	192	64+	17–15	8–8	Contact
5593	♂	186	71	17–15	8–8	Contact
24999	?	195	—	—	8–8	Contact
110886	♂	193	76	17–15	8–8	Contact
Type	♂	199	78	17–15	7–8	Contact

Intergradation between *melanocercus* and *orizabensis* is demonstrated by a series of four specimens bearing the locality data Mirador, Veracruz (nos. 25000–3). Two of these are adults; they have the head and the anterior half of the body peculiarly mottled with jet black on a brown ground color; the posterior third of the dorsum is entirely jet black, the tail black above and below; most of the labials are black-edged. This condition is certainly intermediate between that of *melanocercus* and *orizabensis*. The two young are similar, except that light bands are evident on the anterior portion of the body; the bands are broad, covering about two scale lengths, as in *melanocercus*.

It is to be noted that both typical *orizabensis* and typical *melanocercus* occur near this locality, if the data on two specimens, presumably from the environs of Mirador, can be trusted (no. 25093, *melanocercus;* no. 24999, *orizabensis*). Both these specimens are unquestionably identifiable, even though one (*melanocercus*) is a juvenile.

Upon the evidence of these data, and also because an intergrade of *melanocercus* and *erebennus* is available from farther north, it appears reasonable to assume that *melanocercus* is typically a plains species, while *orizabensis* must be restricted to the extensive area of forested foothills in central and

southern Veracruz, from which all specimens with positively known locality data have been taken.

TABLE 7.—SCALE COUNTS IN ORIZABENSIS-MELANOCERCUS INTERGRADES

Number	Sex	Ventrals	Caudals	Scale rows	Supralabials	Antepenultimate labial
25000	♀	199	—	17–15	8–8	Contact
25001	♂	196	74	17–15	8–8	Contact
25002	♂	190	72	17–15	8–8	Contact
25003	♀	191	72	17–15	8–8	Contact

Drymarchon corais erebennus (Cope)

Georgia obsoleta Baird and Girard, Cat. N. Amer. Rept., pp. 158–159. 1853.
Spilotes erebennus Cope, Proc. Acad. Nat. Sci. Philadelphia, 1860: 342 (substitute name for *Georgia obsoleta* Baird and Girard); *idem*, p. 564.
Coluber corais Boulenger (part), Cat. Snakes Brit. Mus. **2**: 31, 1894. (suppresses *Coluber obsoleta* [Baird and Girard], as a homonym of *Coluber obsoletus* Say, making available *erebennus* Cope).

Type locality.—Eagle Pass, Texas.
Diagnosis.—Black above posteriorly, becoming spotted or banded on middle

TABLE 8.—SCALE COUNTS IN EREBENNUS

Number	Sex	Ventrals	Caudals	Scale rows	Supralabials	Antepenultimate labial
A656	♂	189	63+?	17–14	8–8	Contact
1843	♂	189	61	17–14	8–8	Contact
1859	♂	184	59	17–14	8–8	Contact
1862	♂	—	55	17–14	8–8	Contact
1860	♂	186	56+?	17–14	8–8	Contact
15675	♀	186	60	17–14	8–8	Contact
15872	♀	191	65+	17–15	8–8	Contact
16142	♂	183	—	17–15	8–8	Contact
25200	♂	186	65	17–15	8–8	Contact
26439	♀	193	57	17–14	8–8	Contact
32783	♂	183	—	17–14	8–8	Contact
37515	♂	188	59	17–14	8–8	Contact
65165	♂	186	55	17–14	8–8	1 side
82564	♂	188	—	17–14	8–8	1 side
105307	♂	186	—	17–14	8–8	Contact
105308	♂	183	—	17–14	8–8	Contact
110866	♀	192	—	17–15	8–8	Contact
110867	♂	192	—	17–14	8–8	Contact
110868	♀	188	62	17–14	8–8	Contact
110869	♂	187	58	17–14	8–8	Contact

and anterior part of body in adults; subcaudals less than 68 (55 to 65); antepenultimate labial in contact with temporal or postocular or both; scale rows near anus usually 14.

Range.—Central southern Texas south to extreme northern Veracruz and central Hidalgo.[3]

[3] The specimen from Tasquillo, Hidalgo, described by Martín del Campo (Anal. Inst. Biol. Mex. **8**: 264–265 1937) is obviously of this subspecies. Apparently the form extends up the valleys of the Panuco river system, to which the Rio Tula that flows by Tasquillo belongs. On maps the spot appears well within the plateau of Mexico.

Specimens examined.—Twenty, from the following localities: HIDALGO: Km. 332, 5 kilometers south of Chapulhuacán (no. 110868). VERACRUZ: Tuxpán (no. 25200). SAN LUIS POTOSÍ: Huichihuayán (no. 110869). TAMAULIPAS: Hda. La Clementina, 4 miles west of Forlón (nos. 105307–8, 110866–7; EHT-HMS no. 15872); Matamoras (no. 1859). COAHUILA: Sabinas (no. 37515). TEXAS: Brownsville (nos. 1860, 32783); Lower Rio Grande (no. 1843); San Diego (no. 15675); Eagle Pass (no. 1862, type); Cameron County (no. 65165); McAllen (no. 82564); Las Moras Springs, Kinney County (no. 26439); 29 miles north of Brownsville (Kans. Univ. no. 16142); no locality (EHT no. A656).

Remarks.—This subspecies is well differentiated from all others, having a unique character in usually possessing 14 scale rows near the anus; it differs from all others except *couperi* in having less than 68 caudals.

An intergrade between this subspecies and *melanocercus* is represented by No. 46447 from Metlatoyuca, Puebla (extreme northeastern corner). The coloration of the specimen is exactly typical of *melanocercus*, but the scutellation is that of *erebennus:* scale rows 17-14; ventrals 186; caudals 63; supralabials 8-8; antepenultimate labial in contact with temporal; female.

TABLE 9.—SCALE COUNTS IN COUPERI

Number	Sex	Ventrals	Caudals	Scale rows	Supralabials	Antepenultimate labial
4457	♂	185	66	17–15	7–8	Separated
4458	?	—	—	—	7–8	Separated
4504	♀	186	63	17–15	8–8	Separated
10379	♂	186	67	17–15	8–8	Separated
10465	♀	195	64	17–15	8–8	Separated
10790	♂	188	65	17–15	8–8	Separated
10824	♀	193	64	17–15	8–8	Separated
14842	♂	187	66	17–15	7–8	Separated
18514	♂	187	64	17–15	8–8	Separated
24605	♂	187	65	17–15	8–8	Separated
26618	♂	187	65	17–15	8–8	Separated
36481	♂	186	67	17–15	8–8	Separated
37354	?	—	—	—	8–8	Separated
38101	♂	185	67	17–15	7–8	Separated
38153	?	—	—	—	7–8	Separated
38367	♀	193	63	17–15	8–8	Separated
38579	♂	189	—	17–15	7–7	Separated
38683	♂	187	—	17–15	8–8	Separated
44187	♂	187	—	17–15	7–8	Separated
44519	?	—	—	—	7–7	Separated
61218	♂	186	—	17–15	8–8	Separated
83317	♂	187	67	17–15	8–8	Separated
85307	♂	187	—	17–15	8–8	Separated
85308	♂	189	64	17–15	8–8	Separated
85309	♂	185	66	17–15	8–8	Separated

In color, the subspecies perhaps most easily confused with *erebennus* is *rubidus;* the latter, however, has the back uniform black in adults, and is not spotted anteriorly on dorsal surface; also, the light areas on the lips are white or pink, sharply differentiated from the black (brown in *erebennus*).

Drymarchon corais couperi (Holbrook)

Coluber couperi Holbrook, N. Amer. Herp., ed. 2, **3**: 75, pl. 16. 1842.
Drymarchon corais couperi Stejneger and Barbour, Check List N. Amer. Amph. Rept., ed. 2, p. 93. 1923.

Type locality.—Dry pine hills south of Alatamaha, Ga.

Diagnosis.—Adults uniform black above and below, except gular region; caudals less than 68; antepenultimate labial separated from temporal or postocular by contact above it of adjacent labials; 15 scale rows in front of anus.

Range.—South Carolina to Florida, westward to southern Louisiana (Stejneger and Barbour).

Specimens examined.—Twenty-five. FLORIDA: Silver Springs (Kans. Univ. no. 18514); Lemon City (no. 38153); Kissimee River (no. 36481); West Palm Beach (no. 37354); Gainesville (nos. 10465, 10790, 10824, 14842); Orlando (nos. 26618, 83317); Norwalk ? (nos. 38367, 38683); Clearwater (no. 10379); Pinecrest (nos. 85307–8); Canaveral (no. 44519); Miami (no. 85309); "Florida" (nos. 44187, 24605, 38101, 38579, 61218). GEORGIA: Brunswick (no. 4504); Liberty County (nos. 4457–8).

Remarks.—The existence of a hiatus between the ranges of *couperi* and *erebennus* makes questionable the status of these two as subspecies of the same form. The eastern subspecies, however, is so obviously a derivative of *erebennus*, and their characters in general are so similar, that their relationship is probably best expressed as the name has been used in the past.

This subspecies is the most highly modified of the whole genus. It has a completely evolved, terminal type of color pattern (all black, shared with *orizabensis*), insofar as the trend toward complete melanism is concerned. In addition it possesses three modifications in scutellation, while only one or two modifications occur in other members of the genus: (1) Reduced caudals (shared with *erebennus*); (2) antepenultimate labial separated from temporals and postoculars (unique, almost invariable); and (3) reduction of supralabials to 7 (unique, but in only 20 percent of the counts). Of course, there are changes observable in ventral counts in the various forms of the genus, but the trend in general is so gradual from north to south or vice versa that no one form can be credited with the development of a unique amount or type of variation in this character.

CONCLUSIONS

A number of problems made evident but not solved by the present study may be listed:

1. The existence of other forms, particularly of types more melanistic than *corais*, is to be looked for in South America.

2. The question of intergradation between *corais* and *melanocercus* in South America is still open. Theoretically there should be no intergradation between them, although Amaral (*op. cit.* p. 328) states that "Certain examples from Colombia appear intermediate between *corais corais* and *corais melanurus*."

3. The exact ranges of *melanocercus* and *unicolor*, and the areas of intergradation between them, are yet to be determined.

4. The apparent lack of intergradation, and overlapping of ranges, of *unicolor* and presumed intergrades between *melanocercus* and *rubidus* in southern Chiapas, need verification.

5. There is some evidence that the presumed intergrades between

rubidus and *melanocercus* may be recognizable as a different subspecies, even though its characters undoubtedly have arisen through hybridization between these two forms. Suggestive of this are two specimens from Achotal, Veracruz, in Field Museum of Natural History: one is typical *melanocercus*, the other a typical *melanocercus-rubidus* intergrade; both are adults.

6. The possible split of *melanocercus* into two subspecies should be settled by examination of Honduras and Nicaragua specimens; it is barely possible that *unicolor* extends completely across Nicaragua, in which case an actual separation of a northern and southern population of *melanocercus* is evident.

7. The exact range of *orizabensis* is yet to be defined.

8. The apparent existence of *melanocercus* on the plains of Veracruz north of the Isthmus, indicated by several intergrades between that form and *orizabensis* and *erebennus*, should be verified.

9. The apparent hiatus between the ranges of *erebennus* and *couperi* should be investigated. If these two forms are proved to be separated from each other geographically, their rather sharply different morphological and pattern characters suggest the possibility of considering *couperi* a distinct species.

ZOOLOGY.—*A new brittle-star of the genus* Ophiocomella *from Canton Island.*[1] AUSTIN H. CLARK, U. S. National Museum.

The genus *Ophiocomella* was diagnosed in 1939 with the type species *O. caribbaea*, a small 6-armed form that previously had been considered as the young of *Ophiocoma pumila*. The species assigned to the genus were *Ophiocomella caribbaea*, sp. nov., *O. parva* (H. L. Clark), *O. schmitti*, sp. nov., and *O. clippertoni*, sp. nov. (the last a tentative name for specimens from Clipperton Island doubtfully referred to *O. parva*). The discovery of another species of this curious genus is a matter of considerable interest.

Ophiocomella schultzi, sp. nov.

Description.—The disk is circular, not notched at the arm bases, slightly elevated, 4.3 mm in diameter; the six rather slender arms are 17 mm long; the arms are separated by about three times their basal width. The specimen is sexually mature.

The aboral surface of the disk is covered with fine, overlapping, conspicuously punctate scales. About one-quarter of these scales bear short roughened cylindrical spinelets, which are about twice as high as thick with low-conical or rounded tips. These are rather widely spaced, being usually two to four

[1] Published with the permission of the Secretary of the Smithsonian Institution. Received June 22, 1941.

times their width apart. There are 50 to 60 of these to each square millimeter. The radial shields are visible as small rounded plates between two and three times as long (radially) as broad situated at the edge of the disk, one on each side of the arm base. The edge of the disk is sharp. On the oral side the interradial areas are covered with fine imbricating scales resembling those on the aboral surface but without spinules, these not extending beyond the sharpened edge of the aboral surface where they stop abruptly.

The upper arm plates are fan-shaped, in the earlier portion of the arm about as long as broad. The distal border is approximately hemispherical, somewhat flattened centrally, passing over into the straight lateral edges which converge at an angle of 90°. The proximal angle is rather broadly truncated by the overlapping of the preceding upper arm plate. In the distal portion of the arms the side arm plates encroach more and more on the dorsal surface and finally meet so that in the terminal portion of the arm the upper arm plates, here much reduced in size, are separated by the broad middorsal union of the side arm plates for as much as their own length. The terminal portion of the arm becomes more or less moniliform.

The first side arm plate beyond the edge of the disk has four arm spines, the second five, and those following four, the number falling to three near the arm tip. The uppermost arm spine is about as long as two arm segments, slender, tapering, somewhat flattened, and usually more or less swollen basally and slightly bent distally. On the second arm comb beyond the disk a similar but slightly smaller spine is inserted above the spine corresponding to the uppermost spine on the other plates. The second spine is slightly more slender and slightly shorter than the uppermost. The third spine is about two-thirds the length of the second, tapers somewhat more rapidly, and is slightly curved downward. The lowest spine is slightly more slender than the third and shorter, about the length of an arm segment.

The under arm plates are at first about as long as broad, after about the sixth becoming longer than broad. They are very slightly broader distally than proximally with very broadly rounded distal angles, similarly rounded proximal angles, and slightly concave sides.

The first tentacle pore has two tentacle scales, those following a single rather broad distally pointed scale situated on the side arm plate.

The oral shields are longer than broad, the outer portion approximately hemispherical, the lateral edges converging to a broadly rounded proximal end.

The adoral plates are triangular, the slender produced inner apices extending downward along the sides of the oral shields so as almost or quite to meet the apex of the other of the same pair.

The mouth papillae are four or five in number, well rounded, decreasing in size and in relative width toward the apex of the jaws.

The color of the disk is pale greenish gray with a few rather large indefinite spots of yellow brown; the arms are whitish with occasional indistinct yellow brown blotches.

Locality.—Canton Island, lagoon; collected by Dr. Leonard P. Schultz on April 28, 1939 (U.S.N.M. no. E.5919, type).

Remarks.—This new species is related to *O. schmitti* from which, however, it is quite distinct. The spinules on the disk are finer, more numerous, and much shorter; the upper arm plates are broader and more rounded with the lateral edges making a greater angle with each other; the second side arm plate beyond the disk carries an extra spine aborally; and the oral shields are broader and more rounded.

It seems to differ from *O. parva* (H. L. Clark) from Torres Strait in having the radial shields visible and the granules on the disk more elongated, and in having an extra arm spine on the second side arm plate beyond the disk. In the original description *O. parva* is said to have a single tentacle scale, but the figure shows two on at least two of the first tentacle pores.

Obituaries

MORTON GITHENS LLOYD, distinguished engineer and chief of the Safety Codes Section at the National Bureau of Standards since 1917, died April 26, 1941, at his home in Chevy Chase, Md., after a short illness. Born September 10, 1874, in Beverly, N. J., Dr. Lloyd was educated at the Central Manual Training High School, Philadelphia, and at the University of Pennsylvania, recieving a bachelor of science degree there in 1896, a Ph.D. in 1900 and the E.E. degree in 1908. He also had studied at Harvard University and the Friedrich Wilhelms Universitat, Berlin. Dr. Lloyd was an instructor in physics at the University of Pennsylvania from 1899 to 1902. From the latter year to 1910 he had served as laboratory assistant, assistant physicist, and associate physicist at the Bureau of Standards. He was technical editor of the Electrical Review and Western Electrician, from 1910 to 1916.

During his professional career Dr. Lloyd made special investigations of the effects of self induction and capacity in alternating-current circuits; thermomagnetic and galvanomagnetic effects in bismuth and tellurium; effects of wave form upon induction meters, core loss and ratio of transformers and hysteresis; effects of phases of harmonics upon quality of sound; measurement of hysteresis and eddy currents; magnetic hysteresis in rotary field; regulation of public utilities, accident prevention; and lightning.

Dr. Lloyd took a prominent part in many national associations. He was a fellow of the American Institute of Electrical Engineers, a member of the Washington Academy of Sciences, the American Association of Engineers, United States National Committee of the International Commission of Illumination, president of the International Association of Electrical Inspectors, member of Franklin Institute, Federal Interdepartmental Safety Council, Federal Accident Statisticians, American Association for Labor Legislation, Philosophical Society of Washington, National Fire Protection Association, National Safety Council, past president of the American Society of Safety Engineers, Safety Code Correlating Committee of the American Standards Association, and was an honorary member of the International Municipal Signal Association. He was also a member of the International Electrical Congress, St. Louis, 1904, and Turin, 1911; the International Engineering Congress, San Francisco, 1915, and the International Congress on Illumination, Saranac, N. Y., 1928.

He was elected a member of the honor research fraternity, Sigma Xi. He received a medal from the Louisiana Purchase Exposition, 1904, and was the recipient of the Edward Longstreth Medal of the Franklin Institute, 1910. Dr. Lloyd was the author of numerous technical articles. His writings have been published in bulletins of the Bureau of Standards, Electrical Review and Western Electrician, Electrical World, Proceedings of the A.I.E.E., Proceedings of the International Association of Municipal Elec-

tricians, Journal of the Franklin Institute, Safety Engineering, and Proceedings of the International Association of Electrical Inspectors.

Dr. Lloyd belonged to All Souls Unitarian Church and was a past president of the community association of section three, Chevy Chase, Md. On June 20, 1907, Dr. Lloyd married Miss Ethel Tucker Maurer of Washington, D. C. He is survived by his widow, a daughter, and a son.

WILLIAM LASH MILLER, C.B.E., professor emeritus at the University of Toronto, died on September 1, 1940. He was born at Galt, Ontario, Canada, on September 10, 1866. He attended the University of Toronto, where he was granted an A.B. degree in 1887. He subsequently studied at the Universities of Berlin, Göttingen, Munich, and Leipzig, and obtained the degree of doctor of philosophy from the University of Munich in 1890. Professor Miller was a member of the staff of the University of Toronto for 48 years. After having served as fellow and demonstrator, he was appointed associate professor of physical chemistry in 1900, professor in 1908, head of the department of chemistry in 1921, and was retired as professor emeritus in 1937. In 1935 he was made a Commander of the Order of the British Empire.

Professor Miller made many important contributions to chemical thermodynamics, especially in the field of electrochemistry. He was author of more than 100 original publications, including several comprehensive mathematical papers relating to the kinetics of surface reactions, diffusion, colloidal behavior, and electrochemical phenomena. His review of the *Method of Willard Gibbs in chemical thermodynamics*, published in Chemical Reviews for 1925, exemplifies his most obvious desire to serve his fellow chemists by bringing to their attention the wealth of information to be derived by application of the thermodynamic method. His contributions were not restricted to physicochemical and mathematical investigations, but included fundamental discoveries in other fields, among which may be mentioned the isolation of inositol from Wilder's bios, and the demonstration that inositol is a growth factor for yeasts.

Professor Miller's outstanding ability and wide interest in the development of science brought him many honors and responsibilities in scientific organizations. He served the Journal of Physical Chemistry as member of the board of reviewers from 1896 to 1910 and as associate editor from 1910 to 1926. He was chairman of the chemistry section of the Association for the Advancement of Science in 1913 and in 1923. An honorary member of the American Chemical Society, he served as chairman of the section of physical chemistry in 1906 and as associate editor of the Journal of the American Chemical Society from 1913 to 1924. Professor Miller was one of the founders of the Canadian section of the Society of Chemical Industry and served as chairman in 1910. He was an honorary member of the Electrochemical Society and was elected president in 1912. He was also a member of Franklin Institute, an honorary member of the Electroplaters Association, Fellow of the Royal Society of Canada, serving as president in 1935, a member of the Canadian Institute of Chemistry, serving as president in 1926, and a member of the British Association for the Advancement of Science which he served as vice-president in 1924. He was elected to membership in the Washington Academy of Sciences in October, 1903.